Article

# Discovery of Aminopiperidine Indoles That Activate the Guanine Nucleotide Exchange Factor SOS1 and Modulate RAS Signaling

Jason R. Abbott, Timothy R. Hodges, R Nathan Daniels, Pratiq A. Patel, Jack Phillip Kennedy, Jennifer E. Howes, Denis T. Akan, Michael C. Burns, Jiqing Sai, Tammy Sobolik, Yugandhar Beesetty, Taekyu Lee, Olivia W. Rossanese, Jason Phan, Alex G. Waterson, and Stephen W. Fesik

*J. Med. Chem.*, **Just Accepted Manuscript** • DOI: 10.1021/acs.jmedchem.8b00360 • Publication Date (Web): 01 Jun 2018

# Discovery of Aminopiperidine Indoles That Activate the Guanine Nucleotide Exchange Factor SOS1 and Modulate RAS Signaling

Jason R. Abbott,[◊,#] Timothy R. Hodges,[◊,#] R. Nathan Daniels,[◊,†] Pratiq A. Patel,[◊,‡] J. Phillip Kennedy,[◊,⊥] Jennifer E. Howes,[◊] Denis T. Akan,[◊] Michael C. Burns,[◊,Ω] Jiqing Sai,[◊] Tammy Sobolik,[◊,¶] Yugandhar Beesetty,[◊] Taekyu Lee,[◊] Olivia W. Rossanese,[◊,£] Jason Phan,[◊] Alex G. Waterson,[§,¥] and Stephen W. Fesik[◊,§,¥,*]

[◊]Department of Biochemistry, Vanderbilt University School of Medicine, Nashville, Tennessee 37232-0146, USA

[§]Department of Pharmacology, Vanderbilt University School of Medicine, Nashville, Tennessee 37232-0146, USA

[¥]Department of Chemistry, Vanderbilt University, Nashville, Tennessee 37232-0146, USA

ABSTRACT: Deregulated RAS activity, often the result of mutation, is implicated in approximately 30% of all human cancers. Despite this statistic, no clinically successful treatment for RAS-driven tumors has yet been developed. One approach for modulating RAS activity is to target and affect the activity of proteins that interact with RAS, such as the guanine nucleotide exchange factor (GEF) son of sevenless homologue 1 (SOS1).

Here, we report on structure–activity relationships (SAR) in an indole series of compounds. Using structure-based design, we systematically explored substitution patterns on the indole nucleus, the pendant amino acid moiety, and the linker unit that connects these two fragments. Best-in-class compounds activate the nucleotide exchange process at sub-micromolar concentrations in vitro, increase levels of active RAS-GTP in HeLa cells, and elicit signaling changes in the mitogen-activated protein kinase/extracellular regulated kinase (MAPK/ERK) pathway, resulting in a decrease in pERK1/2$^{T202/Y204}$ protein levels at higher compound concentrations.

## ■ INTRODUCTION

Proteins in the RAS family control an array of important cellular processes, including differentiation, proliferation, and survival.[1-3] Cycling between an active GTP-bound state and an inactive GDP-bound state, these proteins relay signals from cell surface receptors to intracellular signaling pathways.[4-8] Aberrations in RAS signaling can confer upon cells many of the hallmarks of cancer, such as uncontrolled proliferation, avoidance of apoptosis, induction of angiogenesis, and evasion of immune destruction.[9-11] Mutationally activated RAS proteins are implicated in approximately 30% of all human cancers, with the highest incidences occurring in tumors of the pancreas, colon, and lung.[11-13]

Despite the significance of RAS in the field of oncology, the development of a therapeutic means for targeting oncogenic RAS has met with limited success. While direct inhibition is the most straightforward approach, accomplishing this via traditional drug discovery strategies has proven to be a formidable challenge.[14-23] An alternative approach is to target proteins that regulate RAS activity, such as the guanine nucleotide

exchange factor (GEF) son of sevenless homologue 1 (SOS1).[24-26] GEFs promote RAS activation by catalyzing the exchange of GDP for intracellular GTP. During the nucleotide exchange process, RAS engages in a protein–protein interaction with SOS1 and forms a complex (RAS:SOS1:RAS) containing one molecule of SOS1 and two molecules of RAS—one bound to the allosteric site on SOS1 and one bound to the catalytic site (CDC25 domain) on SOS1.[27]

Recently, our laboratory reported on compounds derived from an aminopiperidine indole scaffold that bind to the CDC25 domain of SOS1, adjacent to the Switch II region of RAS in the RAS:SOS1:RAS complex. This binding event stimulates nucleotide exchange on RAS in vitro and increases the levels of RAS-GTP in cancer cells.[24,28] Paradoxically, compound-mediated activation of nucleotide exchange results in the inhibition of downstream extracellular regulated kinase (ERK1/2) phosphorylation through negative feedback on SOS1.[28]

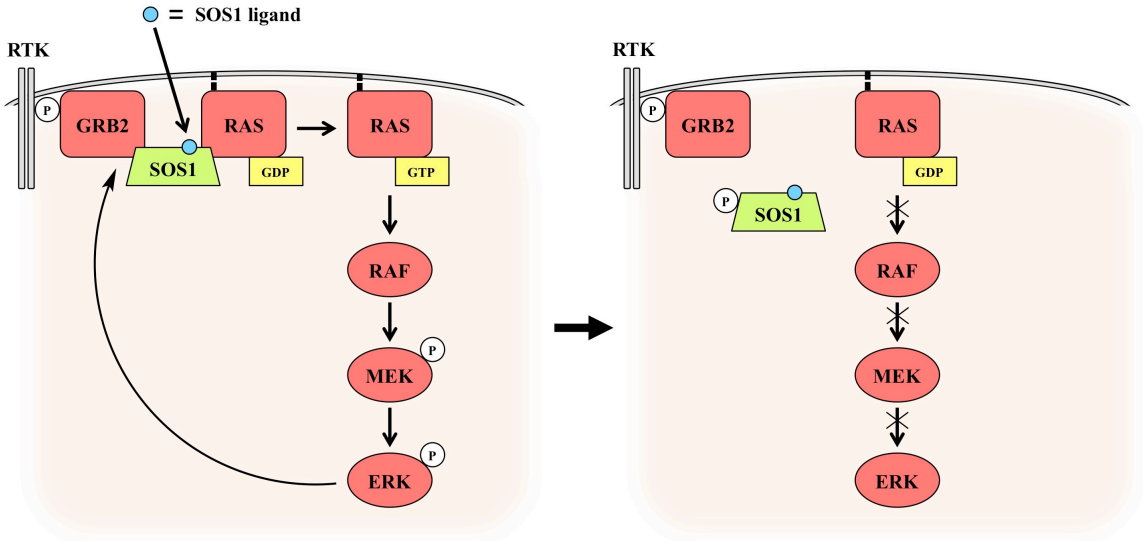


**Figure 1.** Mechanistic hypothesis for the action of SOS1-binding indole compounds.

In the proposed biological mechanism, depicted in Figure 1, binding of an indole compound (SOS1 ligand) to SOS1 increases the rate of nucleotide exchange on RAS. Consequently, the levels of active RAS-GTP increase within the cell, which amplifies signaling down the RAS/RAF/MEK/ERK pathway, and increases the levels of phosphorylated ERK1/2 (pERK1/2$^{T202/Y204}$) protein. Via a negative feedback loop, pERK1/2$^{T202/Y204}$ then phosphorylates SOS1 at Ser1178. This phosphorylation event disrupts the interaction between SOS1 and growth factor receptor bound protein 2 (GRB2), likely delocalizing SOS1 from the vicinity of RAS. As a result, the levels of RAS-GTP decrease, RAS signaling is dampened, and the levels of pERK1/2$^{T202/Y204}$ decrease.[28]

At the time that we first proposed this mechanism, only a few compounds from the indole series were sufficiently potent to induce biphasic signaling changes in cells. To further explore our mechanistic hypothesis, we required more active compounds. Here, we describe the design and synthesis of the aminopiperidine indole compounds that were used in our initial biological studies.[24,28] We further describe the synthesis of more advanced, structurally related analogues that demonstrate markedly improved potency in vitro relative to the first-generation aminopiperidine indoles and, importantly, are more active in a cellular context. We used a structure-based design approach to assess the effects of various substituents on the indole ring system, examine an assortment of amino acid and non-amino acid subunits, and investigate the linker unit that ties these two pieces together. Optimized compounds activate nucleotide exchange at sub-micromolar concentrations in vitro, increase the levels of RAS-GTP in HeLa cells, and elicit biphasic modulation of ERK1/2 phosphorylation.

## ■ RESULTS AND DISCUSSION

**Chemistry.** The general strategies developed for compound synthesis are described in Schemes 1–5. The synthesis of compounds devoid of substitution on the indole nucleus (**4a**–**k**, Table 1) started from the commercially available 1*H*-indole carbaldehyde **1** (Scheme 1). Reductive amination with *tert*-butyl piperidin-4-ylcarbamate, followed by acid-mediated removal of the *N*-Boc protecting group gave amine **2**. Coupling of **2** with carboxylic acids **3a**–**k** furnished the aminopiperidine indole analogues **4a**–**k** shown in Table 1.

**Scheme 1. Synthesis of Compounds 4a–k**[a]

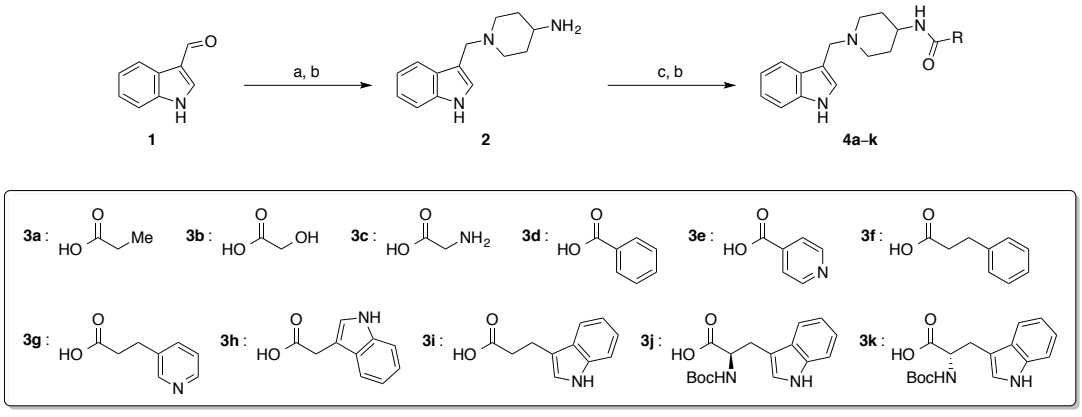


[a]Reagents and conditions: (a) *tert*-Butyl piperidin-4-ylcarbamate, $NaBH(OAc)_3$, DCM. (b) TFA, DCM. (c) **3a**–**k**, PyBOP, *i*-$Pr_2NEt$, DMSO or **3a**–**k**, HATU, *i*-$Pr_2NEt$, DMF.

Analogues substituted on the indole ring were prepared as shown in Scheme 2. The substituted 1*H*-indole carbaldehydes **5a**–**k** were advanced through a four step sequence comprising: (1) reductive amination, (2) *N*-Boc deprotection, (3) coupling with (*tert*-butoxycarbonyl)-L-tryptophan, and (4) *N*-Boc deprotection. The aminopiperidine indole analogues **7a**–**k** depicted in Table 2 were thus obtained.

**Scheme 2. Synthesis of Compounds 7a–k**[a]

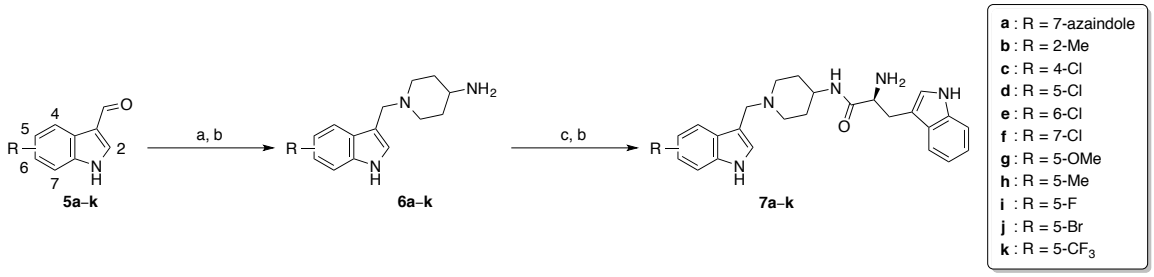


[a]Reagents and conditions: (a) *tert*-Butyl piperidin-4-ylcarbamate, $NaBH(OAc)_3$, DCM. (b) TFA, DCM or 4 M HCl in dioxane, DCM. (c) (*tert*-Butoxycarbonyl)-L-tryptophan, PyBOP, *i*-$Pr_2NEt$, DMSO or (*tert*-Butoxycarbonyl)-L-tryptophan, HATU, *i*-$Pr_2NEt$, DMF.

The synthesis of indole analogues featuring substituted tryptophan moieties (**12a**–**h**, Table 3) was enabled by chemistry developed by Jia and Zhu (Scheme 3).[29] Commercially available anilines **8a**–**h** were elaborated to the tryptophan methyl esters **10a**–**h** via palladium-catalyzed annulation with (*S*)-2-*N*,*N*-di-(*tert*-butoxycarbonyl)-5-oxopentanoate **9**. Hydrolysis of methyl esters **10a**–**h** gave the corresponding carboxylic acids **11a**–**h**, which were advanced to analogues **12a**–**h** via coupling with amine **6d** and deprotection of the two *N*-Boc protecting groups from the tryptophan subunit.

**Scheme 3. Synthesis of Compounds 12a–h**[a]

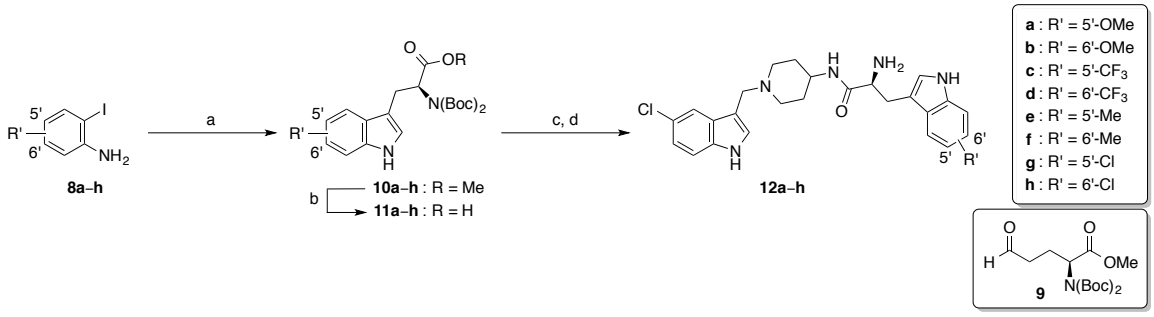


[a]Reagents and conditions: (a) **9**, $Pd(OAc)_2$, DABCO, DMF, 85 °C. (b) KOH,

THF/EtOH/$H_2O$ (1:1:1 v/v/v), 50 °C. (c) **6d**, HATU, *i*-$Pr_2NEt$, DMF. (d) TFA, DCM.

For the synthesis of compounds containing various linker units (**15a**–**f**, Table 4 and **16**–**19**, Table 5), 5-chloro-1*H*-indole-3-carbaldehyde **5d** was subjected to reductive amination with mono-*N*-Boc-diamines **13a**–**f**, and the products treated with TFA to give subunits **14a**–**f** (Scheme 4). Coupling of **14a**–**f** with (*tert*-butoxycarbonyl)-L-tryptophan, followed by *N*-Boc deprotection gave the unsubstituted tryptophan–indoles **15a**–**f** displayed in Table 4. Similarly, compounds **16**–**19**, which comprise the final matrix depicted in Table 5, were prepared via the union of amines **14d** and **14f** with carboxylic acids **11f** and **11h** (Scheme 5).

**Scheme 4. Synthesis of Compounds 15a–f**[a]

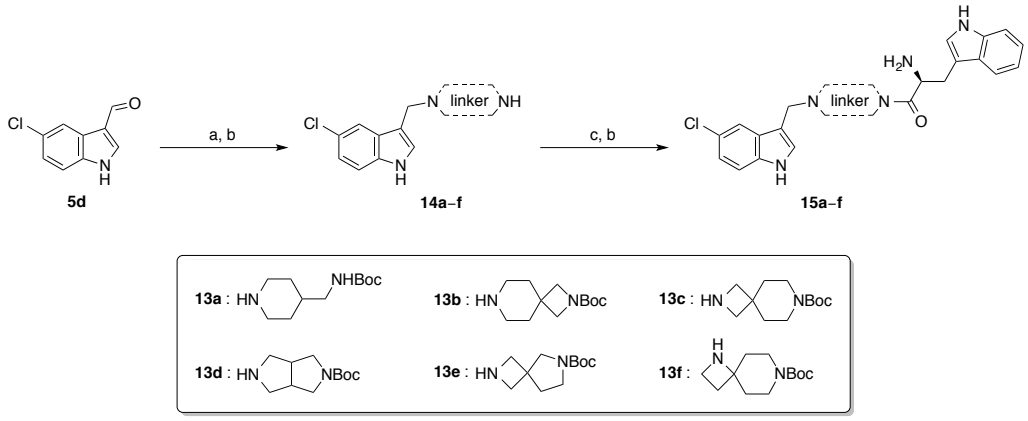


[a]Reagents and conditions: (a) **13a**–**f**, $NaBH(OAc)_3$, DCM. (b) TFA, DCM. (c) (*tert*-Butoxycarbonyl)-L-tryptophan, PyBOP, *i*-$Pr_2NEt$, DMSO.

**Scheme 5. Synthesis of Compounds 16–19**[a]

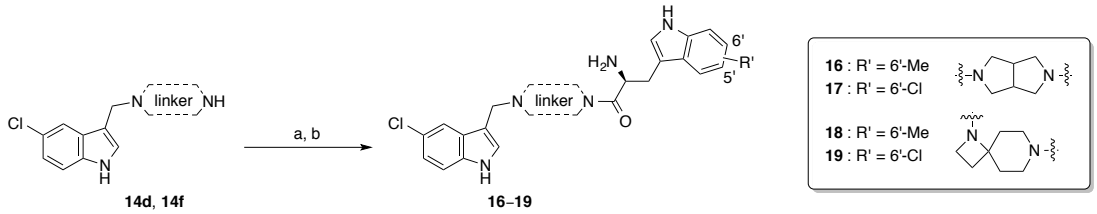

[a]Reagents and conditions: (a) **11f** or **11h**, HATU, *i*-$Pr_2NEt$, DMF. (b) TFA, DCM.

**Compound Design.** *Aminopiperidine Indole Extensions.* The first set of analogues was designed to evaluate extensions from the exocyclic amine of the aminopiperidine unit initially identified as the minimum pharmacophore necessary for nucleotide exchange activation. Accordingly, a variety of amino acid and non-amino acid aminopiperidine amides—a selection of which are shown in Table 1—were synthesized. The ability of these compounds to affect SOS1-mediated nucleotide exchange was assessed using a high throughput nucleotide exchange assay.[24,30] Compound efficacy in vitro was expressed in terms of maximal percent activation (Max. Act. %), defined as the maximum exchange rate elicited by an individual compound at 100 μM relative to the DMSO vehicle control alone. We hypothesized that compounds should elicit a marked increase in the maximum rate of nucleotide exchange in order to modulate RAS-GTP signaling and achieve enhanced potency in cancer cells, as previously discussed.[30] In vitro compound potency was defined as the half maximal effective concentration ($EC_{50}$), calculated from the concentration response curve (0–100 μM compound) generated from the nucleotide exchange assay.

**Table 1. SAR of the Aminopiperidine Extension[a]**

| Compd | Structure | $EC_{50}$ (μM)[b] | Max. Act. (%)[c] |
|---|---|---|---|
| **2** | 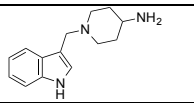 | — | 222 ± 52.2 |
| **4a** | 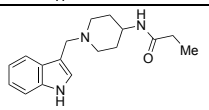 | — | 157 ± 38.8 |
| **4b** | 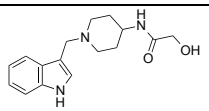 | — | 200 ± 62.0 |

| | | | |
|---|---|---|---|
| **4c** | 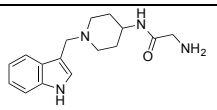 | — | 225 ± 48.1 |
| **4d** | 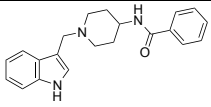 | — | 323 ± 222.0 |
| **4e** | 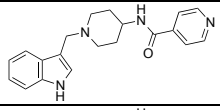 | — | 110 ± 4.7 |
| **4f** | 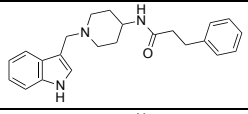 | — | 263 ± 134.4 |
| **4g** | 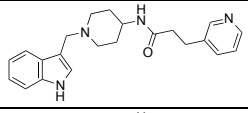 | — | 67 ± 7.2 |
| **4h** | 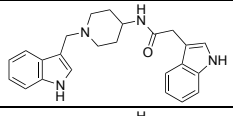 | — | 170 ± 20.6 |
| **4i** | 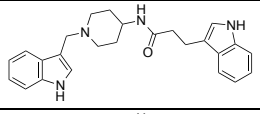 | — | 585 ± 304.3 |
| **4j** | 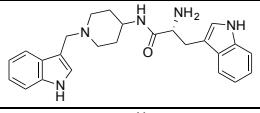 | — | 311 ± 90.8 |
| **4k** | 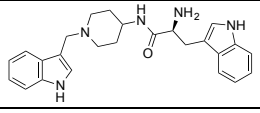 | 89.7 ± 12.34 | 641 ± 225.3 |

[a]Values reported as the mean ± SD of at least two separate experiments.

[b] "—" denotes an $EC_{50}$ value of >100 μM, or an $EC_{50}$ value that was not calculated due to low efficacy in vitro.

[c]Activation values represent percentage relative to DMSO control at a ligand concentration of 100 μM.

Most of the initial analogues, exemplified by **4a**–**c** in Table 1, only weakly stimulated SOS1-catalyzed nucleotide exchange at the maximum evaluated ligand concentration (100 μM), and reliable $EC_{50}$ values could not be derived from the resulting concentration response curves. However, many of these derivatives possessed adequate solubility profiles for use in X-ray crystallographic studies, from which the X-ray structure of glycine analogue **4c** bound to the RAS:SOS1:RAS complex was obtained (Figure 2).[24]

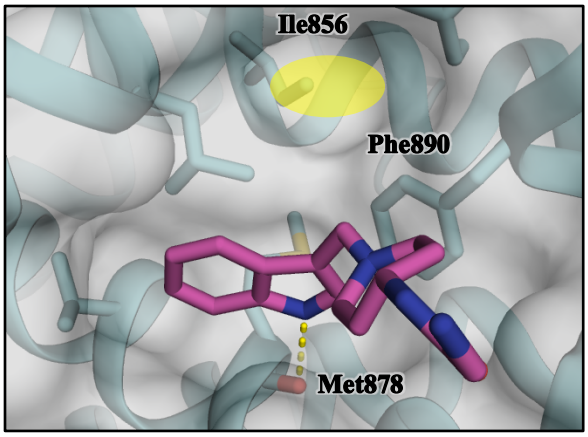


**Figure 2.** X-ray co-crystal structure of compound **4c** (violet; PDB ID code 4NYJ) bound to SOS1 (aqua) in the RAS:SOS1:RAS ternary complex. Yellow circle highlights hydrophobic subpocket above Phe890, near Ile856.

As illustrated in Figure 2, a hydrogen bond between the indole N–H and the backbone carbonyl of Met878 anchors compound **4c** deep within the hydrophobic binding pocket of SOS1. The aminopiperidine linker extends outward, orienting the terminal glycine moiety toward the solvent. In the crystallized binding pose, compound **4c** leaves a nearby hydrophobic subpocket above Phe890 and next to Ile856 unoccupied (Figure 2, yellow circle). We hypothesized that increasing the ligand's occupation of this region would potentially enhance the potency of these early stage compounds. Thus, several aminopiperidine amides featuring aromatic side-chains were synthesized (**4d**–**k**, Table 1). The majority of these new derivatives showed no measureable improvement in the nucleotide exchange assay. However, compound **4k**, which features a tryptophan subunit, activated the nucleotide exchange process to a desirably high maximal rate as compared to the other compounds tested in Table 1 (Max. Act. = 641%), and with an $EC_{50}$ of 89.7 μM.[24] Although similar to **4k** in structure, compounds **4i** and **4j**—the

deamino and enantiomeric analogues of compound **4k**, respectively—showed reduced nucleotide exchange activity.

To guide the next round of optimization, an X-ray structure of compound **4k** bound to SOS1 in the RAS:SOS1:RAS complex was obtained (Figure 3).[24] Similar to the glycine analogue **4c**, compound **4k** retains a hydrogen bond with the backbone carbonyl group of Met878. The aminopiperidine linker extends out from the binding pocket and folds back on itself, positioning the tryptophan arene ring close to the hydrophobic subpocket formed by Ile856, Phe890, and Ile893. In the crystallized binding pose, the tryptophan N–H sits in close proximity to Glu902, and engages in a hydrogen bond with the carboxylate side-chain of this residue.

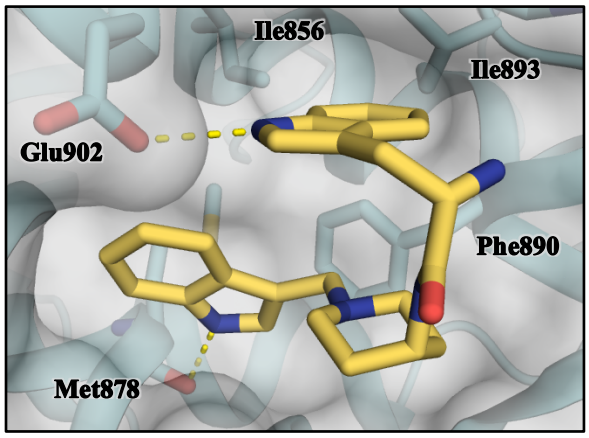


**Figure 3.** X-ray co-crystal structure of compound **4k** (gold; PDB ID code 4NYM) bound to SOS1 (aqua) in the RAS:SOS1:RAS ternary complex.

*SAR of the Indole Ring System.* The X-ray co-crystal structure shown in Figure 3, combined with the data in Table 1, suggested that additional improvements in potency could be realized by refining three areas of the compound: (1) the indole anchor, (2) the aromatic ring of the tryptophan subunit, and (3) the aminopiperidine linker connecting these two pieces. In an attempt to fill the unoccupied space around the indole ring system,

analogues with substituents at the 2-, 4-, 5-, 6-, and 7-positions of the indole nucleus were prepared (Table 2). Within this iteration of compounds, a preference for substitution at C-5 of the indole ring system emerged. This is exemplified by the 9-fold improvement in potency of the 5-chloroindole **7d** over the 5*H*-indole **4k**. Conversely, 4-, 6-, and 7-chloroindoles—**7c**, **7e**, and **7f**—demonstrated reduced potency and diminished efficacy compared to compound **4k**.

In addition to compound **7d**, other 5-substituted indoles demonstrated improved potency relative to the 5*H*-indole **4k** in the nucleotide exchange assay. These include the 5-methyl analogue **7h**, the 5-bromo analogue **7j**, and the 5-trifluoromethyl analogue **7k**, which exhibited $EC_{50}$ values of 29.2, 14.2, and 11.2 μM, respectively. Consistent with the hydrophobic nature of the binding pocket, the 5-methoxy derivative **7g** and the azaindole **7a** demonstrated reduced activity. Finally, the 2-methylindole **7b** was also only weakly active, suggesting that substitution at this position was not well tolerated.

**Table 2. SAR of the Indole Ring System**[a]

| Compd | Structure | $EC_{50}$ (μM)[b] | Max. Act. (%)[c] |
|---|---|---|---|
| **4k** | 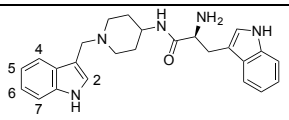 | 89.7 ± 12.34[31] | 641 ± 225.3 |
| **7a** | 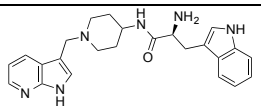 | — | 86 ± 3.6 |
| **7b** | 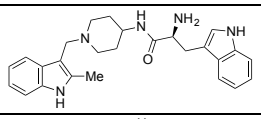 | — | 159 ± 13.9 |
| **7c** | 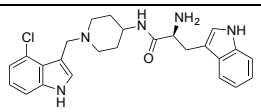 | — | 259 ± 60.6 |
| **7d** | 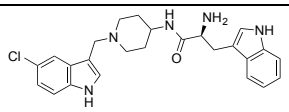 | 9.6 ± 4.27 | >1000 |

| | | | |
|---|---|---|---|
| **7e** | 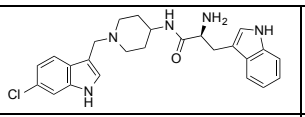 | — | 250 ± 53.0 |
| **7f** | 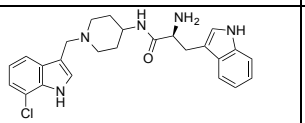 | — | 146 ± 28.6 |
| **7g** | 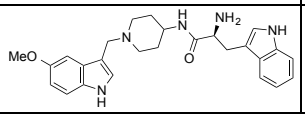 | — | 813 ± 429.4 |
| **7h** | 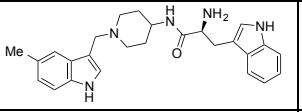 | 29.2 ± 5.39 | >1000 |
| **7i** | 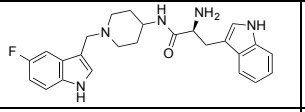 | 15.9 ± 2.30 | 158 ± 15.9 |
| **7j** | 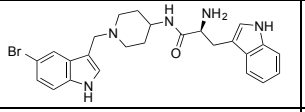 | 14.2 ± 3.58 | >1000 |
| **7k** | 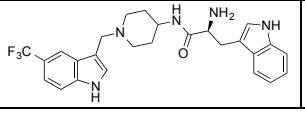 | 11.2 ± 0.25 | 407 ± 24.1 |

[a]Values reported as the mean ± SD of at least two separate experiments.

[b] "—" denotes an $EC_{50}$ value of >100 μM, or an $EC_{50}$ value that was not calculated due to low efficacy in vitro.

[c]Activation values represent percentage relative to DMSO control at a ligand concentration of 100 μM.

To explore other areas of the molecule, we chose to fix the indole scaffold upon which to build further SAR. The 5-chloroindole **7d** was chosen for its improved potency and efficacy relative to the other compounds in Table 2, and for its greater ligand efficiency (LE) and lipophilic efficiency (LipE) (LE = 0.22; LipE = 1.62) relative to other 5-substitued indoles, such as the 5-bromoindole **7j** (LE = 0.21; LipE = 1.37) and the 5-(trifluoromethyl)indole **7k** (LE = 0.20; LipE = 1.28).[32-34]

Prior to the discovery of compound **7d**, activation values in the nucleotide exchange assay were reported as maximal percent activation (Max. Act. %), relative to the DMSO vehicle control. Although this format was useful for identifying hit compounds in the nucleotide exchange assay, a degree of variability in the baseline activation rate was noted between different experiments. Thus, to allow for more reliable

comparison of activation values between plates, compound **7d** was included as an internal control in every subsequent nucleotide exchange experiment. Compound efficacy was then expressed in terms of relative nucleotide exchange activation (Rel. Act. %), which was calculated as the percentage of maximal activation elicited by a given compound at 100 μM, normalized to the maximal activation elicited by compound **7d** at 100 μM. As discussed in a recent publication, compounds that achieved greater than approximately 50% relative activation in vitro elicited a more robust induction of RAS-GTP levels in a cellular context.[30] This threshold was subsequently used to predict whether or not a given compound was likely to produce activity in cells.

*SAR of the Tryptophan Ring System.* With the identity of the indole anchor established and the reporting of activation values standardized, the focus shifted to the optimization of the tryptophan subunit and the aminopiperidine linker. These two areas of chemical space were investigated in parallel using the data for compound **7d** as a baseline for comparison. Analysis of the X-ray co-crystal structure of compound **4k** shown in Figure 3 suggested that the tryptophan moiety did not adequately fill the hydrophobic subpocket above Phe890, near Ile856. This area did, however, appear to be accessible from the aromatic ring of the tryptophan nucleus. As such, a series of substituted tryptophan derivatives were prepared and tested in the nucleotide exchange assay. As shown in Table 3, compounds **12a** and **12c**–**h**—substituted at either the 5'- or 6'-position of the tryptophan ring—all showed improved potency in vitro relative to the parent compound **7d**, while also achieving similar levels of efficacy. Within this series of analogues, the data for matched pairs of C-5'- and C-6'-substituted tryptophans indicated a preference for substitution at the 6'-position (**12c** versus **12d**; **12e** versus **12f**; and **12g**

versus **12h**). Most notable was compound **12h**, which exhibited an $EC_{50}$ value of 1.4 μM—7-fold more potent than its predecessor **7d**.

**Table 3. SAR of the Tryptophan Ring System**[a]

| Compd | Structure | $EC_{50}$ (μM) | Rel. Act. (%)[b] |
|---|---|---|---|
| **7d** | 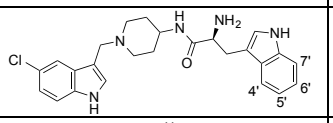 | 9.6 ± 4.27 | 100 |
| **12a** | 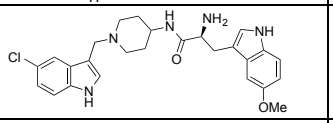 | 8.5 ± 0.21 | 105 ± 20.8 |
| **12b** | 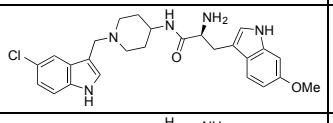 | 15.1 ± 8.66 | 87 ± 24.6 |
| **12c** | 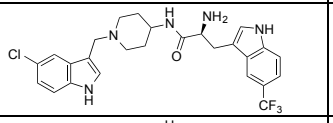 | 7.8 ± 4.76 | 72 ± 31.3 |
| **12d** | 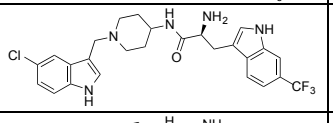 | 6.1 ± 2.45 | 105 ± 28.1 |
| **12e** | 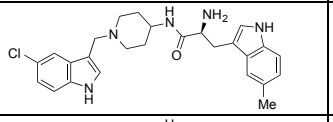 | 5.9 ± 1.96 | 104 ± 32.7 |
| **12f** | 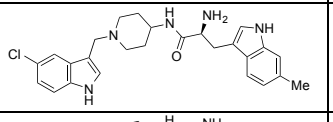 | 3.1 ± 1.04 | 120 ± 29.5 |
| **12g** | 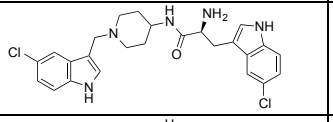 | 1.6 ± 0.40 | 87 ± 19.7 |
| **12h** | 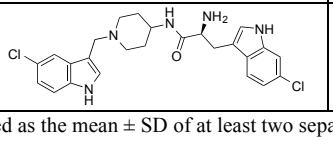 | 1.4 ± 0.09 | 107 ± 36.4 |

[a]Values reported as the mean ± SD of at least two separate experiments.

[b]Activation values calculated as the percentage activation for each compound at 100 μM relative to the activation of control compound **7d** at 100 μM.

From a structural perspective, the preference for substitution at the 6'-position of the tryptophan ring system can be rationalized by overlaying the X-ray co-crystal structures of the regioisomeric matched pairs **12e** versus **12f** and **12g** versus **12h** bound to SOS1 in the RAS:SOS1:RAS ternary complex (Figure 4a,b). As shown in Figure 4a, the

chlorine atom at the 6'-position of the tryptophan nucleus in compound **12h** fits into the hydrophobic pocket near Ile856 (Figure 4a–c, yellow circle). Conversely, the chlorine atom of its 5'-regioisomer **12g** floats above this pocket and is not well ordered in the crystal structure. Figure 4b shows the same observation to be true for the methyl analogues **12e** and **12f**, however the 6'-methyl group on compound **12f** does extend as deeply into the binding pocket as the corresponding 6'-chlorine atom on compound **12h** (Figure 4c). In addition to more adequately filling the hydrophobic space near Ile856, the 6'-chlorotryptophan **12h** engages several residues in the binding pocket, including Met878 via a direct H–bond, and Asp887 via two separate water-mediated interactions (Figure 4d).

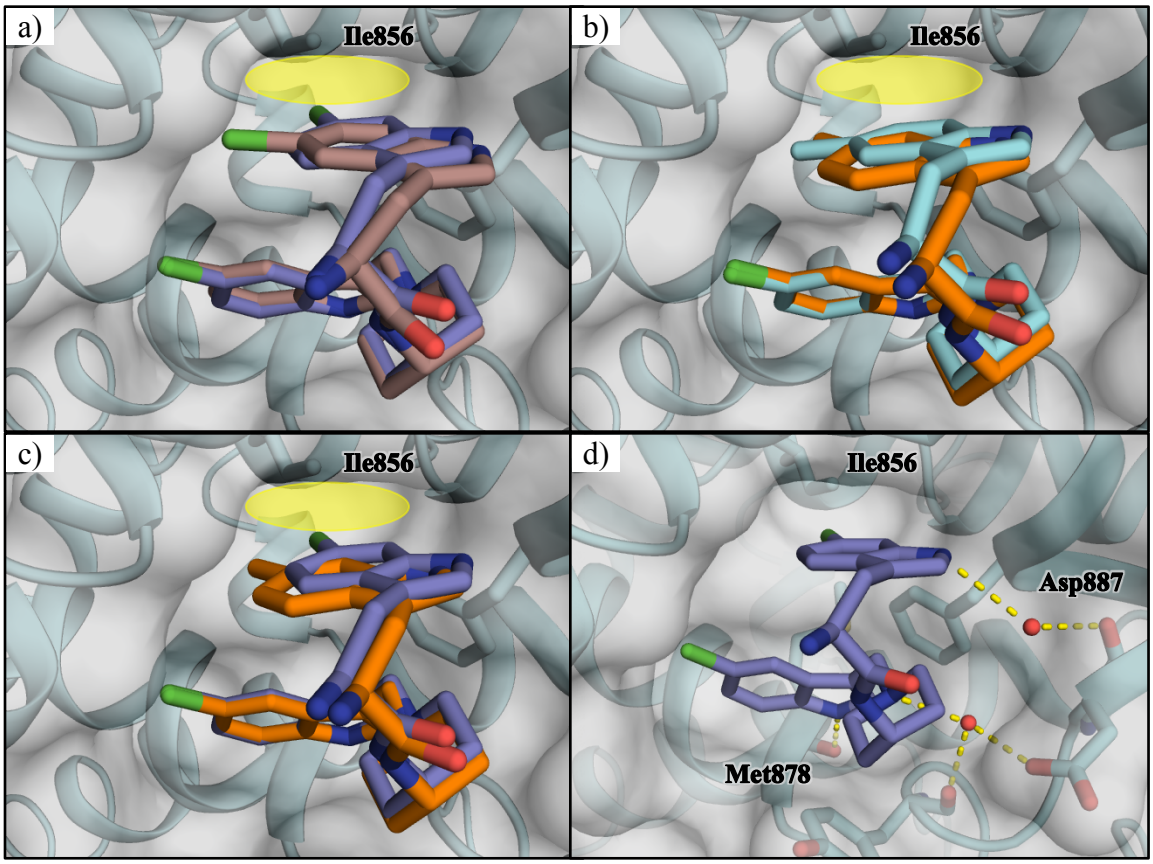


**Figure 4.** (a) Overlay of compounds **12g** (salmon; PDB ID code 6BVJ) and **12h** (purple; PDB ID code 6BVI). (b) Overlay of compounds **12e** (cyan; PDB ID code 6BVL) and **12f**

(orange; PDB ID code 6BVK). (c) Overlay of compounds **12f** (orange) and **12h** (purple). Yellow circle highlights the hydrophobic pocket near Ile856. (d) X-ray co-crystal structure of compound **12h** (purple) bound to SOS1 (aqua) in the RAS:SOS1:RAS ternary complex.

*Aminopiperidine Replacements.* In parallel to the compounds in Table 3, analogues of compound **7d** were designed in which the 5-chloroindole and the tryptophan subunits were connected through a variety of linker moieties. As shown earlier in Figure 3, the aminopiperidine ring of compound **4k** adopts a U-shaped configuration upon binding to SOS1, which is approximately 34 kcal/mol higher in energy than the ground state conformation of the ligand, calculated using water as the solvent (see Supporting Information). We hypothesized that reinforcing the binding conformation of the ligand would potentially reduce the entropic penalty of binding.[35-37] Thus, a focused set of compounds featuring rigidified cyclic and bicyclic amine linkers was synthesized (Table 4), exemplified by compound **15d**, for which the difference in energy between the ground state conformation and a conformation resembling that of the bound ligand is approximately 29 kcal/mol, calculated using water as the solvent (see Supporting Information).

The compounds featuring rigidified linker units were then tested in the nucleotide exchange assay, where analogues **15d–f** proved to be more potent than the comparator compound **7d** (Table 4). On the other hand, compounds **15b** and **15c**, both of which feature the 2,7-diazaspiro[3.5]nonane linker, were less potent and less efficacious in vitro than compound **7d**. Finally, introducing additional flexibility into the linker unit (e.g. compound **15a**) did not greatly affect compound activity.

**Table 4. SAR of the Diamine Linker Unit**[a]

| Compd | Structure | $EC_{50}$ (μM)[b] | Rel. Act. (%)[c] |
|---|---|---|---|
| **7d** | 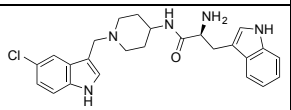 | 9.6 ± 4.27 | 100 |
| **15a** | 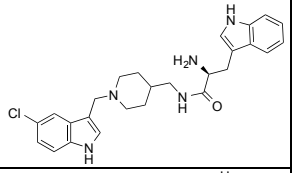 | 13.3 ± 5.69 | 82 ± 40.9 |
| **15b** | 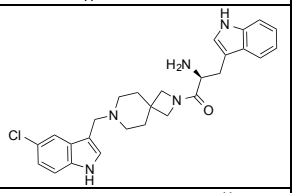 | — | 44 ± 15.3 |
| **15c** | 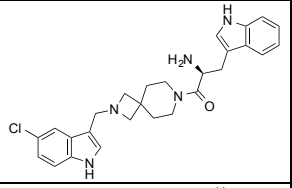 | 37.3 ± 18.36 | 35 ± 9.2 |
| **15d** | 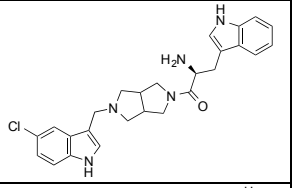 | 6.7 ± 2.61 | 76 ± 3.1 |
| **15e** | 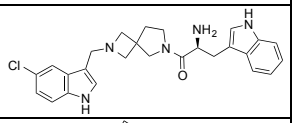 | 4.5 ± 1.84 | 150 ± 37.2 |
| **15f** | 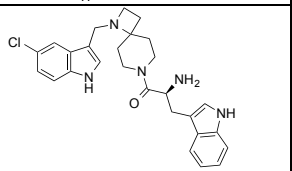 | 2.9 ± 0.29 | 97 ± 34.1 |

[a]Values reported as the mean ± SD of at least two separate experiments.

[b]"—" denotes an $EC_{50}$ value of >100 μM, or an $EC_{50}$ value that was not calculated due to low efficacy in vitro.

[c]Activation values calculated as the percentage activation for each compound at 100 μM relative to the activation of control compound **7d** at 100 μM.

As Figure 5a illustrates, the octahydropyrrolo[3,4-*c*]pyrrole ring system within compound **15d** orients the tryptophan moiety into the back of the binding pocket in a similar manner as the aminopiperidine linker of the initial lead compound **4k**. In the crystallized binding pose, compound **15d** engages in a water-mediated interaction with

Tyr884 and Asp887, and a water-mediated interaction with the backbone carbonyl of Phe890 (Figure 5b). Together, these interactions, coupled with the rigidified ligand conformation, likely explain the improved potency of compound **15d** vis-à-vis compound **4k**.

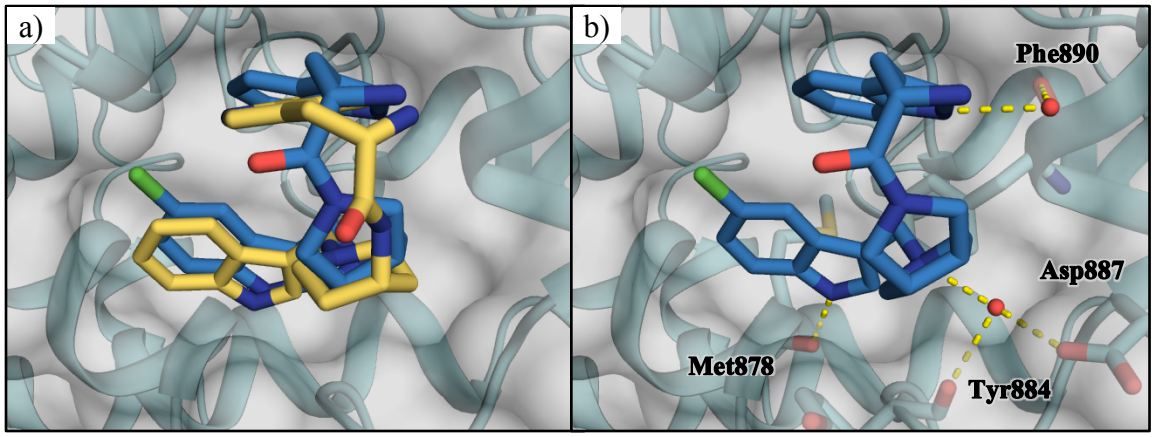


**Figure 5.** (a) Overlay of compounds **15d** (marine; PDB ID code 6BVM) and **4k** (gold; PDB ID code 4NYM). (b) X-ray co-crystal structure of compound **15d** (marine) bound to SOS1 (aqua) in the RAS:SOS1:RAS ternary complex.

Having realized potency improvements by adding substituents to the tryptophan ring system and by changing the aminopiperidine linker separately, we sought to combine these two structural modifications in an effort to achieve further improvements in compound activity. Towards this end, the compounds shown in Table 5 were synthesized. These compounds each feature one of the preferred 6'-substituted tryptophan motifs combined with one of the preferred linker units. Incorporation of these two design elements into a single molecule generated the most potent compounds to date in the indole series. Compounds **17**–**19** activated SOS1-catalyzed nucleotide exchange above the relative activation threshold and with $EC_{50}$ values below 1.0 μM.

**Table 5. SAR of Optimized Compounds**[a]

| Compd | Structure | $EC_{50}$ (μM) | Rel. Act. (%)[b] |
|---|---|---|---|
| **16** | 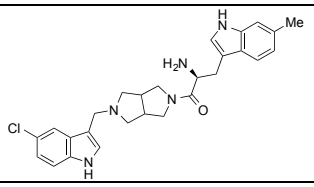 | 4.4 ± 1.61 | 123 ± 8.8 |
| **17** | 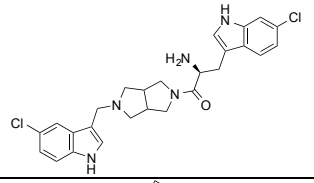 | 0.8 ± 0.47 | 119 ± 16.3 |
| **18** | 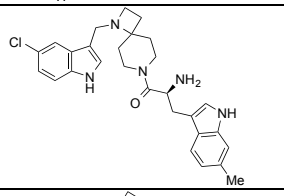 | 0.8 ± 0.09 | 105 ± 32.8 |
| **19** | 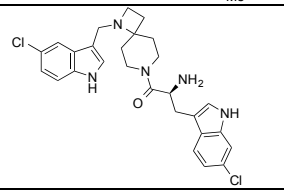 | 0.8 ± 0.36 | 78 ± 23.3 |

[a]Values reported as the mean ± SD of at least two separate experiments.

[b]Activation values calculated as the percentage activation for each compound at 100 μM relative to the activation of control compound **7d** at 100 μM.

**Biological Evaluation.** In order to determine whether the improvements in biochemical potency translated to enhanced cellular potency, the cellular effects on RAS-GTP and pERK1/2$^{T202/Y204}$ protein levels that were elicited by four compounds with a range of $EC_{50}$ values were measured (Figure 6). To facilitate comparison between these compounds—**12h**, **15c**, **17**, and **19**—quantification values for RAS-GTP and pERK1/2$^{T202/Y204}$ levels normalized to their respective controls are provided below each blot. These numbers are also provided in the Supporting Information (Tables S1 and S2), along with quantification data for compound **7d**, which was used in previous mechanistic studies, and served as the control compound in the nucleotide exchange assay (vide supra).[24,28] Importantly, the trends in RAS-GTP and pERK1/2$^{T202/Y204}$ modulation were consistent between independent biological replicates (Tables S1 and S2).

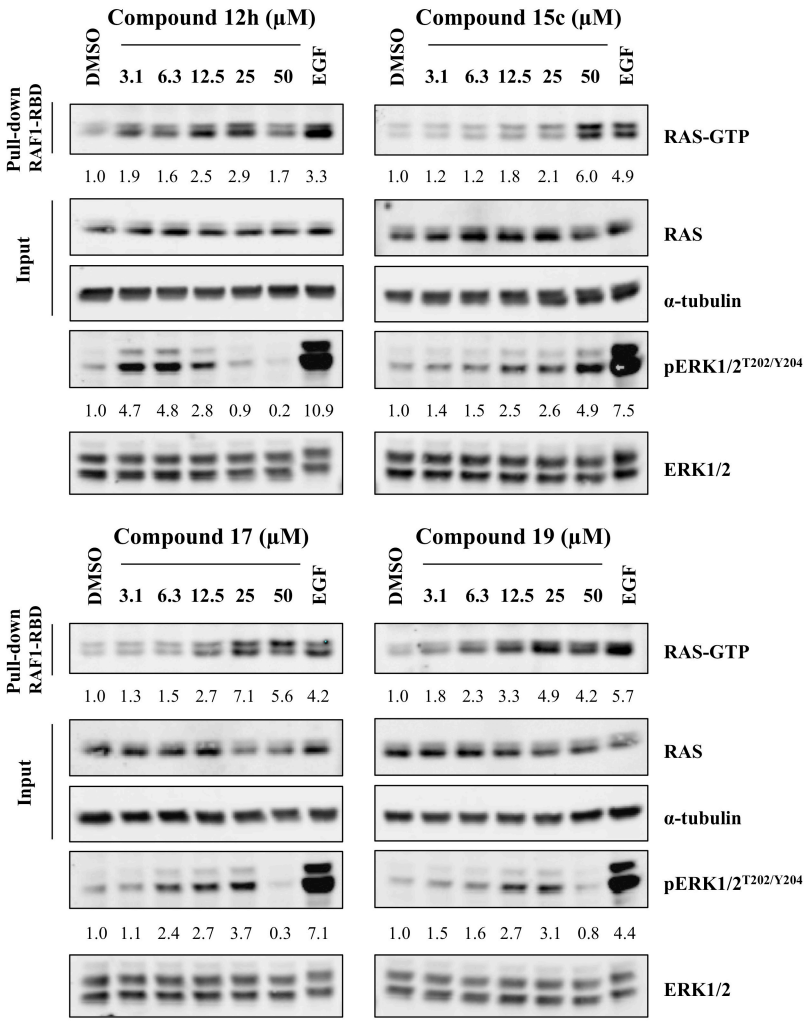


**Figure 6.** RAS-GTP and corresponding pERK1/2$^{T202/Y204}$ levels from HeLa cells that were treated for 30 min with up to 50 μM of compounds **12h**, **15c**, **17**, or **19**. EGF treatment (50 ng/mL for 5 min) was used as a positive control for pathway activation. Quantification values for RAS-GTP levels and pERK1/2$^{T202/Y204}$ levels are displayed under their respective blots for each compound. The levels of RAS-GTP were normalized to the total RAS protein levels and to the DMSO control. The levels of pERK1/2$^{T202/Y204}$ were normalized to the total ERK1/2 protein levels and to the DMSO control. Data are representative of two independent experiments.

Previously, it was reported that compound **7d** ($EC_{50}$ = 9.6 μM**)** stimulates maximum production of RAS-GTP at 50 μM, after a 30 min treatment in HeLa cells.[24,28] Relative to compound **7d**, compounds **12h**, **17**, and **19** exhibit lower $EC_{50}$ values in vitro ($EC_{50}$ = 1.4, 0.8, and 0.8 μM, respectively). As illustrated in Figure 6, in HeLa cells, compounds **12h**, **17**, and **19** cause dose-dependent increases in RAS-GTP at treatment concentrations as low as 3.1 μM, and a peak in RAS-GTP levels at 25 μM. In line with the biochemical assay results, which showed compound **15c** to be less potent ($EC_{50}$ = 37.3 μM) than compounds **12h**, **17**, and **19**, higher treatment concentrations of compound **15c** were required to activate RAS-GTP production.

In addition to modulating the levels of RAS-GTP, compounds **12h**, **17**, and **19** also reduced the levels of pERK1/2$^{T202/Y204}$ below baseline at concentrations of 25–50 μM (Figure 6). On the other hand, neither compound **7d** nor compound **15c** inhibited ERK1/2 phosphorylation over the concentration range tested (0–50 μM, Table S2). Thus, compounds **12h**, **17**, and **19** achieved a higher potency of pERK1/2$^{T202/Y204}$ inhibition than both compounds **7d** and **15c**.

Taken together, these findings further articulate our recently proposed mechanism for the modulation of RAS signaling, wherein compound-induced increases in the levels of RAS-GTP produce biphasic modulation of ERK1/2 phosphorylation via negative feedback on SOS1 by pERK1/2$^{T202/Y204}$.[28] The results displayed in Figure 6 (and in Tables S1 and S2) also suggest that improvements in biochemical potency generated through SAR optimization led to compounds with enhanced potency for RAS-GTP activation and pERK1/2$^{T202/Y204}$ inhibition in HeLa cells.

## ■ CONCLUSION

In this study, we have described the structure-based design and synthesis of a series of SOS1-binding indole compounds. By systematically exploring three different areas of the initial lead molecule **4k**—the arene ring of the indole, the amino acid extension, and the linker unit—we discovered the most potent compounds in this indole series, **17**–**19**. These compounds exhibit sub-micromolar activation of SOS1-catalyzed nucleotide exchange on RAS in vitro. In HeLa cells, compounds **17** and **19** increase the levels of RAS-GTP and cause biphasic modulation of ERK1/2 phosphorylation, characterized by an increase in the levels of pERK1/2$^{T202/Y204}$ at lower compound concentrations and a decrease in the levels of pERK1/2$^{T202/Y204}$ below baseline at higher compound concentrations. Notably, potency improvements realized in vitro translated to enhanced potency in HeLa cells, relative to previously reported compounds from this series.[24] These findings are consistent with our recent mechanistic studies demonstrating that compound-mediated activation of RAS results in biphasic modulation of ERK1/2 phosphorylation through negative feedback on SOS1; thus, it is likely that these compounds modulate RAS signaling through the same biological mechanism.[28] This series of indole-derived compounds provides a unique opportunity to explore SOS1-mediated RAS-dependent signaling and to establish the therapeutic implications of modulating RAS activity through SOS1 in cancer cells.

## ■ EXPERIMENTAL SECTION

**General Procedures.** All chemical reagents and reaction solvents were purchased from commercial suppliers and used as received. Proton nuclear magnetic resonance ($^1$H

NMR) spectra were recorded at either 400 MHz or 600 MHz on a Bruker spectrometer. For $^1$H NMR spectra, chemical shifts are reported in parts per million (ppm) and are reported relative to residual non-deuterated solvent signals. Coupling constants are reported in hertz (Hz). The following abbreviations (or a combination, thereof) are used to describe splitting patterns: s, singlet; d, doublet; t, triplet; q, quartet; quint, quintet; m, multiplet; comp, overlapping multiplets of non-magnetically equivalent protons; br, broad. All compounds were of 95% purity or higher, unless otherwise noted, as measured by analytical reversed-phase HPLC. Analytical HPLC was performed on an Agilent 1200 series system with UV detection at 214 and 254 nm, along with evaporative light scattering detection (ELSD). Low-resolution mass spectra were obtained on an Agilent 6140 mass spectrometer with electrospray ionization (ESI). LC-MS experiments were performed with the following parameters: Phenomenex Kinetex 2.6 μm XB-C18 100 Å, LC column 50 x 2.1 mm; 2 min gradient, 5%–95% MeCN in $H_2O$, and 0.1% TFA or 0.1% formic acid. Analytical thin layer chromatography (TLC) was performed on Kieselgel 60 $F_{254}$ glass plates precoated with a 0.25 mm thickness of silica gel. TLC plates were visualized with UV light and iodine. Silica gel chromatography was performed using a Teledyne Isco Combiflash® Rf system. Preparative reversed-phase HPLC was performed on a Gilson instrument equipped with a Phenomenex Kinetex C18 column, using varying concentrations of MeCN in $H_2O$, and 0.1% TFA.

The synthesis of and characterization data for compounds **2**, **4c**, **4k**, **7d**, and **7h** has been reported previously.[24]

**General Procedure 1—Reductive Amination of 1*H*-Indole Carbaldehydes 1 and 5a–k for the Synthesis of Amines 2, 6a–k, and 14a–f**

STEP 1: Similar to the previously reported procedure,[24] a mono-*N*-Boc-diamine (1.00 equiv) and a 1*H*-indole carbaldehyde, such as **1** or **5a**–**k** (1.10 equiv), were dissolved in DCM (0.3 M). The solution was stirred for 0.25–3 h before sodium triacetoxyborohydride ($NaBH(OAc)_3$) (2.00 equiv) was added. The progress of the reaction was monitored by LC-MS analysis. When the reaction was complete, the mixture was diluted with saturated aqueous sodium bicarbonate ($NaHCO_3$) until pH ≈ 7 was achieved. The resulting mixture was diluted with water ($H_2O$) and the organic layer was collected. The aqueous phase was extracted with three portions of DCM. The organic phases were combined, concentrated in vacuo, and purified by silica gel chromatography to give the *N*-Boc-(1*H*-indol-3yl)methanamines.

STEP 2: A mixture of an *N*-Boc-(1*H*-indol-3yl)methanamine (1.00 equiv) and DCM/TFA (9:1 v/v) (0.2 M) or DCM/4 M HCl in dioxane (3:1 v/v) (0.1 M) was stirred at room temperature. The progress of the reaction was monitored by LC-MS analysis. When the reaction was complete, the mixture was concentrated in vacuo. The residue was either azeotroped with toluene three times and the product amine **2**, **6a**–**k**, or **14a**–**f** used directly as its corresponding salt, or dissolved in methanol, rotated with MP-carbonate, filtered, and concentrated to give the amine **2**, **6a**–**k**, or **14a**–**f** as its free base.

**General Procedure 2—Synthesis of Compounds 4a–b, 4i–j, 7c, 7e–g, 7i–k, and 15a–f**

STEP 1: An amine or amine salt, such as **2**, **6a**–**k**, or **14a**–**f** (1.00 equiv), and (benzotriazol-1-yloxy)tripyrrolidinophosphonium hexafluorophosphate (PyBOP) (1.10 equiv) were dissolved in DMSO (0.25 M). The solution was stirred at room temperature. A carboxylic acid (1.00 equiv) and *N*,*N*-diisopropylethylamine (*i*-$Pr_2NEt$) (2.00 equiv)

were added. The progress of the reaction was monitored by LC-MS analysis. When the reaction was complete, the mixture was directly purified by reversed-phase preparative HPLC. The target compound was then obtained as its free base by passage through an Isolute® SCX-2 cartridge or by treatment with MP-carbonate.

STEP 2: If necessary, a mixture of the coupled product obtained in STEP 1 (1.00 equiv) and DCM/TFA (9:1 v/v) (0.2 M) was stirred at room temperature. The progress of the reaction was monitored by LC-MS analysis. When the reaction was complete, the mixture was concentrated in vacuo. The residue was purified by reversed-phase preparative HPLC. The target compound was then obtained as its free base by passage through an Isolute® SCX-2 cartridge or by treatment with MP-carbonate.

**General Procedure 3—Synthesis of Compounds 4d–h and 7a–b**

STEP 1: A carboxylic acid (1.00 equiv) was dissolved in DMF (0.3 M). Next, 1-[bis(dimethylamino)methylene]-1*H*-1,2,3-triazolo[4,5-*b*]pyridinium 3-oxid hexafluorophosphate (HATU) (1.10 equiv) and *i*-$Pr_2NEt$ (3.00 equiv) were added. The resulting mixture was stirred for 15 min at room temperature before a solution of an amine or amine salt, such as **2**, **6a**–**k**, or **14a**–**f** (1.0 M in DMF) (1.10 equiv), was added. After 18 h, the reaction mixture was diluted with ethyl acetate (EtOAc) and washed successively with 1 M citric acid, saturated aqueous $NaHCO_3$, and brine. The organic phase was dried over sodium sulfate ($Na_2SO_4$) and concentrated in vacuo. The residue was purified by reversed-phase preparative HPLC. The target compound was then obtained as its free base by passage through an Isolute® SCX-2 cartridge.

STEP 2: If necessary, a mixture of the coupled product obtained in STEP 1 and DCM/4 M HCl in dioxane (3:1 v/v) (0.1 M) was stirred at room temperature. The progress of the reaction was monitored by LC-MS analysis. When the reaction was complete, the mixture was concentrated in vacuo. The residue was purified by reversed-phase preparative HPLC. The target compound was then obtained as its free base by passage through an Isolute® SCX-2 cartridge.

**General Procedure 4—Synthesis of Compounds 12a–h and 16–19**

STEP 1: According to the procedure reported by Jia and Zhu,[29] (*S*)-2-*N*,*N*-di-*tert*-butoxycarbonyl-5-oxopentanoate **9** (1.00 equiv), an aniline, such as **8a**–**h** (1.10 equiv), palladium(II) acetate ($Pd(OAc)_2$) (0.10 equiv), and DABCO (3.00 equiv) were added to a reaction vial. The vial was sealed, evacuated, and refilled with nitrogen ($N_2$). The evacuation/refill cycle was repeated two additional times. Degassed DMF (0.3 M) was then added and the reaction mixture was heated to 85 °C. After 18 h, the reaction mixture was cooled to room temperature and then diluted with $H_2O$ and EtOAc. The resulting emulsion was treated with sodium chloride (NaCl) and the layers were separated. The aqueous phase was extracted with two portions of EtOAc. The organic phases were combined, washed with brine, dried over $Na_2SO_4$, and concentrated in vacuo. The residue was purified by silica gel chromatography to provide the tryptophan methyl esters **10a**–**h**.

STEP 2: A tryptophan methyl ester, such as **10a**–**h** (1.00 equiv), was dissolved in a mixture of THF/ethanol (EtOH)/$H_2O$ (1:1:1 v/v/v) (0.05 M). Powdered potassium hydroxide (KOH) (8.00 equiv) was added and the mixture was heated to 50 °C. After 6 h, the mixture was cooled to room temperature and concentrated in vacuo. The residue was

partitioned between $H_2O$ and diethyl ether ($Et_2O$). The organic layer was discarded and the aqueous phase was acidified to pH ≈ 4–5 with 2.5 M citric acid before being extracted with three portions of EtOAc. The organic phases were combined, washed with brine, dried over $Na_2SO_4$, and concentrated in vacuo. The residue was purified by silica gel chromatography to give the tryptophan carboxylic acids **11a**–**h**.

STEP 3: A tryptophan carboxylic acid, such as **11a**–**h** (1.00 equiv), was dissolved in DMF (0.4 M). Next, HATU (1.10 equiv) and *i*-$Pr_2NEt$ (3.00 equiv) were added. The resulting mixture was stirred for 15 min at room temperature before a solution of an amine or amine salt, such as **2**, **6a**–**k**, or **14a**–**f** (0.2 M in DMF) (1.10 equiv) was added. After 18 h, the reaction mixture was diluted with EtOAc and washed successively with 1 M citric acid, saturated aqueous $NaHCO_3$, and brine. The organic phase was dried over $Na_2SO_4$ and concentrated in vacuo. The residue was used without further purification.

STEP 4: The coupled product obtained in STEP 3 (1.00 equiv) was dissolved in DCM (0.05 M) and stirred at room temperature. Next, TFA (0.2 M) was added and the mixture was stirred for 2 h before being concentrated in vacuo. The residue was purified by reversed-phase preparative HPLC. The target compound was then obtained as its free base by passage through an Isolute® SCX-2 cartridge.

***N*-(1-((1*H*-Indol-3-yl)methyl)piperidin-4-yl)propionamide (4a).** Prepared from 1*H*-indole-3-carbaldehyde, *tert*-butyl piperidin-4-ylcarbamate, and propionic acid according to general procedure 1 followed by general procedure 2 (70% yield over three steps). Glassy solid. $^1$H NMR (400 MHz, DMSO-$d_6$, δ): 10.90 (br s, 1H), 7.62 (d, $J$ = 7.8 Hz, 2H), 7.34 (d, $J$ = 7.9 Hz, 1H), 7.20 (d, $J$ = 1.7 Hz, 1H), 7.06 (dd, $J$ = 7.2, 0.9 Hz, 1H),

6.97 (dd, $J$ = 7.2, 0.6 Hz, 1H), 3.61 (s, 2H), 3.51–3.47 (m, 1H), 2.84 (d, $J$ = 11.0 Hz, 2H), 2.02 (q, $J$ = 7.5 Hz, 2H), 2.00 (br s, 2H), 1.67 (d, $J$ = 12.4 Hz, 2H), 1.39–1.29 (m, 2H), 0.96 (t, $J$ = 7.5 Hz, 3H). MS (ESI) *m/z* = 286.30 $[M+H]^+$. LC-MS $^t$R (UV 214): 0.728 min.

***N*-(1-((1*H*-Indol-3-yl)methyl)piperidin-4-yl)-2-hydroxyacetamide (4b).** Prepared from 1*H*-indole-3-carbaldehyde, *tert*-butyl piperidin-4-ylcarbamate, and 2-hydroxyacetic acid according to general procedure 1 followed by general procedure 2 (59% yield over three steps). Glassy solid. $^1$H NMR (400 MHz, DMSO-$d_6$, δ): 10.97 (br s, 1H), 7.64 (d, $J$ = 7.8 Hz, 1H), 7.52 (d, $J$ = 7.0 Hz, 1H), 7.35 (d, $J$ = 8.0 Hz, 1H), 7.25 (s, 1H), 7.07 (t, $J$ = 7.4 Hz, 1H), 6.98 (t, $J$ = 7.5 Hz, 1H), 5.38 (t, $J$ = 5.8 Hz, 1H), 3.76 (d, $J$ = 5.6 Hz, 2H), 3.69–3.61 (comp, 3H), 2.89 (br s, 2H), 2.12 (br s, 2H), 1.68 (br d, $J$ = 11.4 Hz, 2H), 1.55–1.47 (m, 2H). MS (ESI) *m/z* = 288.30 $[M+H]^+$. LC-MS $^t$R (UV 214): 0.634 min.

***N*-(1-((1*H*-Indol-3-yl)methyl)piperidin-4-yl)benzamide (4d).** Prepared from 1*H*-indole-3-carbaldehyde, *tert*-butyl piperidin-4-ylcarbamate, and benzoic acid according to general procedure 1 followed by general procedure 3 (12% yield over three steps). White solid. $^1$H NMR (400 MHz, $CD_3OD$, δ): 7.78 (d, $J$ = 8.0 Hz, 2H), 7.65 (d, $J$ = 7.8 Hz, 1H), 7.52–7.48 (m, 1H), 7.45–7.41 (comp, 2H), 7.36 (d, $J$ = 8.1 Hz, 1H), 7.24 (s, 1H), 7.11 (dd, $J$ = 7.1, 1.0 Hz, 1H), 7.04 (dd, $J$ = 7.4, 1.0 Hz, 1H), 3.91–3.83 (m, 1H), 3.79 (s, 2H), 3.08 (d, $J$ = 12.0 Hz, 2H), 2.28 (dd, $J$ = 12.3, 1.7 Hz, 2H), 1.94 (d, $J$ = 12.2 Hz, 2H), 1.69 (qd, $J$ = 12.4, 3.7 Hz, 2H). MS (ESI) *m/z* = 334.30 $[M+H]^+$. LC-MS $^t$R (UV 214): 1.061 min.

***N*-(1-((1*H*-Indol-3-yl)methyl)piperidin-4-yl)isonicotinamide (4e).** Prepared from 1*H*-indole-3-carbaldehyde, *tert*-butyl piperidin-4-ylcarbamate, and isonicotinic acid according to general procedure 1 followed by general procedure 3 (38% yield over three steps). Clear, glassy solid. $^1$H NMR (400 MHz, $CD_3OD$, δ): 8.66 (dd, *J* = 4.6, 1.7 Hz, 2H), 7.75 (dd, *J* = 4.6, 1.7 Hz, 2H), 7.65 (d, *J* = 7.8 Hz, 1H), 7.36 (d, *J* = 8.0 Hz, 1H), 7.23 (s, 1H), 7.11 (dd, *J* = 7.1, 1.0 Hz, 1H), 7.04 (dd, *J* = 7.3, 1.0 Hz, 1H), 3.91–3.83 (m, 1H), 3.79 (s, 2H), 3.07 (d, *J* = 12.0 Hz, 2H), 2.27 (dd, *J* = 11.9, 1.9 Hz, 2H), 1.94 (d, *J* = 12.1 Hz, 2H), 1.67 (qd, *J* = 12.2, 3.7 Hz, 2H). MS (ESI) *m/z* = 335.20 $[M+H]^+$. LC-MS $^t$R (UV 214): 0.799 min.

***N*-(1-((1*H*-Indol-3-yl)methyl)piperidin-4-yl)-3-phenylpropanamide (4f).** Prepared from 1*H*-indole-3-carbaldehyde, *tert*-butyl piperidin-4-ylcarbamate, and 3-phenylpropanoic acid according to general procedure 1 followed by general procedure 3 (22% yield over three steps). Clear, glassy solid. $^1$H NMR (400 MHz, $CD_3OD$, δ): 7.61 (d, *J* = 7.9 Hz, 1H), 7.35 (d, *J* = 8.0 Hz, 1H), 7.25–7.14 (comp, 6H), 7.10 (dd, *J* = 8.0, 1.1 Hz, 1H), 7.03 (dd, *J* = 8.0, 1.0 Hz, 1H), 3.74 (s, 2H), 3.63–3.56 (m, 1H), 2.93 (d, *J* = 11.7 Hz, 2H), 2.87 (t, *J* = 7.8 Hz, 2H), 2.43 (t, *J* = 7.8 Hz, 2H), 2.21 (t, *J* = 11.4 Hz, 2H), 1.75 (dd, *J* = 12.8, 3.1 Hz, 2H), 1.42 (qd, *J* = 11.6, 3.6 Hz, 2H). MS (ESI) *m/z* = 362.20 $[M+H]^+$. LC-MS $^t$R (UV 214): 1.091 min.

***N*-(1-((1*H*-Indol-3-yl)methyl)piperidin-4-yl)-3-(pyridin-3-yl)propanamide (4g).** Prepared from 1*H*-indole-3-carbaldehyde, *tert*-butyl piperidin-4-ylcarbamate, and 3-

(pyridin-3-yl)propanoic acid according to general procedure 1 followed by general procedure 3 (22% yield over three steps). Clear, glassy solid. $^1$H NMR (400 MHz, $CD_3OD$, δ): 8.41 (d, *J* = 4.6 Hz, 1H), 7.71 (td, *J* = 7.7, 1.7 Hz, 1H), 7.64 (d, *J* = 7.8 Hz, 1H), 7.39 (d, *J* = 8.0 Hz, 1H), 7.34 (s, 1H), 7.28 (d, *J* = 7.8 Hz, 1H), 7.22 (dd, *J* = 7.1, 5.0 Hz, 1H), 7.13 (dd, *J* = 7.2, 0.8 Hz, 1H), 7.07 (dd, *J* = 7.4, 0.8 Hz, 1H), 4.01 (s, 2H), 3.72–3.64 (m, 1H), 3.13 (d, *J* = 10.1 Hz, 2H), 3.04 (t, *J* = 7.5 Hz, 2H), 2.60–2.51 (comp, 4H), 1.86 (d, *J* = 11.6 Hz, 2H), 1.60–1.50 (comp, 2H). MS (ESI) *m/z* = 363.10 $[M+H]^+$. LC-MS $^t$R (UV 214): 0.195 min.

**_N_-(1-((1_H_-Indol-3-yl)methyl)piperidin-4-yl)-2-(1_H_-indol-3-yl)acetamide (4h).** Prepared from 1*H*-indole-3-carbaldehyde, *tert*-butyl piperidin-4-ylcarbamate, and 2-(1*H*-indol-3-yl)acetic acid according to general procedure 1 followed by general procedure 3 (4% yield over three steps). Clear, glassy solid. $^1$H NMR (400 MHz, $CD_3OD$, δ): 7.59 (d, *J* = 7.9 Hz, 1H), 7.53 (d, *J* = 7.9 Hz, 1H), 7.34 (d, *J* = 7.7 Hz, 2H), 7.18 (s, 1H), 7.14 (s, 1H), 7.11–7.07 (comp, 2H), 7.04–6.98 (comp, 2H), 3.70 (s, 2H), 3.68–3.64 (m, 1H), 3.61 (s, 2H), 2.89 (d, *J* = 11.0 Hz, 2H), 2.19 (t, *J* = 11.6 Hz, 2H), 1.80 (dd, *J* = 12.9, 3.0 Hz, 2H), 1.53–1.44 (comp, 2H). MS (ESI) *m/z* = 387.30 $[M+H]^+$. LC-MS $^t$R (UV 214): 1.093 min.

**_N_-(1-((1_H_-Indol-3-yl)methyl)piperidin-4-yl)-3-(1_H_-indol-3-yl)propanamide (4i).** Prepared from 1*H*-indole-3-carbaldehyde, *tert*-butyl piperidin-4-ylcarbamate, and 3-(1*H*-indol-3-yl)propanoic acid according to general procedure 1 followed by procedure 2 (71% yield over three steps). Foamy solid. $^1$H NMR (400 MHz, DMSO-$d_6$, δ): 10.89 (br

s, 1H), 10.72 (br s, 1H), 7.70 (d, *J* = 7.7 Hz, 1H), 7.62 (d, *J* = 7.8 Hz, 1H), 7.51 (d, *J* = 7.9 Hz, 1H), 7.33 (d, *J* = 8.1 Hz, 1H), 7.30 (d, *J* = 8.1 Hz, 1H), 7.20 (d, *J* = 2.1 Hz, 1H), 7.08–7.02 (comp, 3H), 6.98–6.93 (comp, 2H), 3.58 (s, 2H), 3.55–3.48 (m, 1H), 2.89 (t, *J* = 7.8 Hz, 2H), 2.81 (d, *J* = 11.0 Hz, 2H), 2.39 (t, *J* = 7.8 Hz, 2H), 1.96 (t, *J* = 11.0 Hz, 2H), 1.66 (d, *J* = 12.4 Hz, 2H), 1.37–1.27 (comp, 2H). MS (ESI) *m/z* = 401.30 $[M+H]^+$. LC-MS $^t$R (UV 214): 0.943 min.

**(*R*)-*N*-(1-((1*H*-Indol-3-yl)methyl)piperidin-4-yl)-2-amino-3-(1*H*-indol-3-yl)propanamide (4j).** Prepared from 1*H*-indole-3-carbaldehyde, *tert*-butyl piperidin-4-ylcarbamate, and (*tert*-butoxycarbonyl)-D-tryptophan according to general procedure 1 followed by general procedure 2 (46% yield over four steps). Glassy solid. $^1$H NMR (400 MHz, DMSO-$d_6$, δ): 10.89 (br s, 1H), 10.81 (br s, 1H), 7.66 (d, *J* = 8.0 Hz, 1H), 7.61 (d, *J* = 7.8 Hz, 1H), 7.54 (d, *J* = 7.8 Hz, 1H), 7.32 (t, *J* = 8.8 Hz, 2H), 7.19 (d, *J* = 2.2 Hz, 1H), 7.12 (d, *J* = 2.2 Hz, 1H), 7.08–7.02 (comp, 2H), 6.98–6.93 (comp, 2H), 3.58 (s, 2H), 3.53–3.45 (m, 1H), 3.41 (dd, *J* = 7.6, 5.5 Hz, 1H), 3.01 (dd, *J* = 14.1, 5.3 Hz, 1H), 2.78–2.73 (comp, 3H), 1.97 (t, *J* = 11.5 Hz, 2H), 1.59 (t, *J* = 13.8 Hz, 2H), 1.36–1.24 (comp, 2H). MS (ESI) *m/z* = 416.20 $[M+H]^+$. LC-MS $^t$R (UV 214): 0.821 min.

**(*S*)-*N*-(1-((1*H*-Pyrrolo[2,3-*b*]pyridin-3-yl)methyl)piperidin-4-yl)-2-amino-3-(1*H*-indol-3-yl)propanamide (7a).** Prepared from 1*H*-pyrrolo[2,3-*b*]pyridine-3-carbaldehyde, *tert*-butyl piperidin-4-ylcarbamate, and (*tert*-butoxycarbonyl)-L-tryptophan according to general procedure 1 followed by general procedure 3 (76% yield over four steps). Tan solid. $^1$H NMR (400 MHz, $CD_3OD$, δ): 8.22 (dd, *J* = 4.8, 1.3 Hz, 1H), 8.12 (dd, *J* = 7.9,

1.4 Hz, 1H), 7.60 (d, *J* = 7.9 Hz, 1H), 7.41 (s, 1H), 7.34 (d, *J* = 8.1 Hz, 1H), 7.17–7.09 (comp, 3H), 7.03 (td, *J* = 7.9, 0.8 Hz, 1H), 3.82 (br s, 2H), 3.72 (t, *J* = 7.0 Hz, 1H), 3.64–3.54 (m, 1H), 3.37 (s, 2H), 3.21–3.09 (m, 2H), 2.95 (br d, *J* = 11.4 Hz, 1H), 2.85 (br s, 1H), 2.35–2.23 (m, 2H), 1.79 (br d, *J* = 12.6 Hz, 1H), 1.51–1.39 (comp, 3H), 1.32–1.20 (m, 2H). MS (ESI) *m/z* = 417.10 $[M+H]^+$. LC-MS $^t$R (UV 214): 0.700 min.

**(*S*)-2-Amino-3-(1*H*-indol-3-yl)-*N*-(1-((2-methyl-1*H*-indol-3-yl)methyl)piperidin-4-yl)propanamide (7b).** Prepared from 2-methyl-1*H*-indole-3-carbaldehyde, *tert*-butyl piperidin-4-ylcarbamate, and (*tert*-butoxycarbonyl)-L-tryptophan according to general procedure 1 followed by general procedure 3 (27% yield over four steps). Clear, glassy solid. $^1$H NMR (400 MHz, $CD_3OD$, δ): 7.57 (d, *J* = 7.9 Hz, 1H), 7.48 (d, *J* = 7.9 Hz, 1H), 7.31 (d, *J* = 8.1 Hz, 1H), 7.23 (d, *J* = 8.1 Hz, 1H), 7.09–6.95 (comp, 5H), 3.62 (s, 2H), 3.55–3.49 (comp, 2H), 3.04 (qd, *J* = 14.0, 7.0 Hz, 2H), 2.87–2.79 (br m, 2H), 2.39 (s, 3H), 2.21–2.12 (m, 2H), 1.67 (br d, *J* = 12.2 Hz, 1H), 1.47 (br d, *J* = 12.2 Hz, 1H), 1.40–1.30 (m, 1H), 1.26–1.17 (m, 1H). MS (ESI) *m/z* = 430.30 $[M+H]^+$. LC-MS $^t$R (UV 214): 0.950 min.

**(*S*)-2-Amino-*N*-(1-((4-chloro-1*H*-indol-3-yl)methyl)piperidin-4-yl)-3-(1*H*-indol-3-yl)propanamide (7c).** Prepared from 4-chloro-1*H*-indole-3-carbaldehyde, *tert*-butyl piperidin-4-ylcarbamate, and (*tert*-butoxycarbonyl)-L-tryptophan according to general procedure 1 followed by general procedure 2 (21% yield over four steps). White solid. $^1$H NMR (600 MHz, $CD_3OD$, δ): 7.58 (d, *J* = 7.8 Hz, 1H), 7.31 (t, *J* = 8.4 Hz, 2H), 7.24 (s, 1H), 7.10–6.98 (comp, 5H), 3.94 (s, 2H), 3.55 (t, *J* = 6.9 Hz, 2H), 3.08 (dd, *J* = 14.2, 7.1

Hz, 1H), 3.01 (dd, *J* = 14.2, 6.6 Hz, 1H), 2.92 (br s, 1H), 2.84 (br s, 1H), 2.24–2.13 (comp, 2H), 1.67 (br d, *J* = 12.8 Hz, 1H), 1.47 (br d, *J* = 12.8 Hz, 1H), 1.40–1.32 (m, 1H), 1.26–1.19 (m, 1H). MS (ESI) *m/z* = 450.00 $[M+H]^+$. LC-MS $^t$R (UV 214 nm): 0.852 min.

**(*S*)-2-Amino-*N*-(1-((6-chloro-1*H*-indol-3-yl)methyl)piperidin-4-yl)-3-(1*H*-indol-3-yl)propanamide (7e).** Prepared from 6-chloro-1*H*-indole-3-carbaldehyde, *tert*-butyl piperidin-4-ylcarbamate, and (*tert*-butoxycarbonyl)-L-tryptophan according to general procedure 1 followed by general procedure 2 (35% yield over four steps). Glassy solid. $^1$H NMR (400 MHz, DMSO-$d_6$, δ): 11.04 (br s, 1H), 10.81 (br s, 1H), 7.65 (d, *J* = 7.9 Hz, 1H), 7.62 (d, *J* = 8.4 Hz, 1H), 7.54 (d, *J* = 7.9 Hz, 1H), 7.38 (d, *J* = 1.8 Hz, 1H), 7.31 (d, *J* = 8.1 Hz, 1H), 7.24 (d, *J* = 2.2 Hz, 1H), 7.12 (d, *J* = 2.2 Hz, 1H), 7.04 (dd, *J* = 7.2, 0.9 Hz, 1H), 6.99–6.93 (comp, 2H), 3.56 (s, 2H), 3.52–3.45 (m, 1H), 3.41 (dd, *J* = 7.6, 5.4 Hz, 1H), 3.33 (br s, 2H), 3.01 (dd, *J* = 14.1, 5.2 Hz, 1H), 2.74 (dd, *J* = 14.1, 7.8 Hz, 1H), 2.75–2.70 (comp, 2H), 1.95 (t, *J* = 11.3 Hz, 2H), 1.58 (t, *J* = 13.2 Hz, 2H), 1.36–1.24 (comp, 2H). MS (ESI) *m/z* = 450.30 $[M+H]^+$. LC-MS $^t$R (UV 214): 0.903 min.

**(*S*)-2-Amino-*N*-(1-((7-chloro-1*H*-indol-3-yl)methyl)piperidin-4-yl)-3-(1*H*-indol-3-yl)propanamide (7f).** Prepared from 7-chloro-1*H*-indole-3-carbaldehyde, *tert*-butyl piperidin-4-ylcarbamate, and (*tert*-butoxycarbonyl)-L-tryptophan according to general procedure 1 followed by general procedure 2 (37% yield over four steps). Glassy solid. $^1$H NMR (400 MHz, DMSO-$d_6$, δ): 11.27 (br s, 1H), 10.82 (br s, 1H), 7.69 (d, *J* = 7.9 Hz, 1H), 7.61 (d, *J* = 7.9 Hz, 1H), 7.55 (d, *J* = 7.9 Hz, 1H), 7.31 (d, *J* = 8.1 Hz, 1H), 7.28 (d,

*J* = 2.3 Hz, 1H), 7.15 (d, *J* = 7.5 Hz, 1H), 7.13 (d, *J* = 2.2 Hz, 1H), 7.04 (dd, *J* = 7.8, 0.9 Hz, 1H), 6.98 (t, *J* = 7.8 Hz, 1H), 6.95 (dd, *J* = 7.8, 0.8 Hz, 1H), 3.59 (s, 2H), 3.54–3.47 (m, 1H), 3.43 (dd, *J* = 7.6, 5.6 Hz, 1H), 3.32 (br s, 2H), 3.02 (dd, *J* = 14.1, 5.4 Hz, 1H), 2.78 (dd, *J* = 14.1, 7.8 Hz, 1H), 2.77–2.71 (comp, 2H), 1.97 (t, *J* = 11.2 Hz, 2H), 1.62–1.54 (comp, 2H), 1.36–1.24 (comp, 2H). MS (ESI) *m/z* = 450.30 $[M+H]^+$. LC-MS $^t$R (UV 214): 0.891 min.

**(*S*)-2-Amino-3-(1*H*-indol-3-yl)-*N*-(1-((5-methoxy-1*H*-indol-3-yl)methyl)piperidin-4-yl)propanamide (7g).** Prepared from 5-methoxy-1*H*-indole-3-carbaldehyde, *tert*-butyl piperidin-4-ylcarbamate, and (*tert*-butoxycarbonyl)-L-tryptophan according to general procedure 1 followed by general procedure 2 (39% yield over four steps). Glassy solid. $^1$H NMR (400 MHz, DMSO-$d_6$, δ): 10.80 (br s, 1H), 10.73 (br s, 1H), 7.62 (d, *J* = 8.0 Hz, 1H), 7.54 (d, *J* = 7.9 Hz, 1H), 7.31 (d, *J* = 8.1 Hz, 1H), 7.22 (d, *J* = 8.7 Hz, 1H), 7.15–7.09 (comp, 3H), 7.04 (t, *J* = 7.3 Hz, 1H), 6.95 (t, *J* = 7.5 Hz, 1H), 6.71 (dd, *J* = 8.7, 2.3 Hz, 1H), 3.74 (s, 3H), 3.54 (s, 2H), 3.52–3.47 (m, 1H), 3.38 (dd, *J* = 7.5, 5.4 Hz, 1H), 3.01 (dd, *J* = 14.0, 5.1 Hz, 1H), 2.78–2.70 (comp, 3H), 1.96 (t, *J* = 11.1 Hz, 2H), 1.66–1.57 (comp, 4H), 1.37–1.24 (comp, 2H). MS (ESI) *m/z* = 446.40 $[M+H]^+$. LC-MS $^t$R (UV 214): 0.810 min.

**(*S*)-2-Amino-*N*-(1-((5-fluoro-1*H*-indol-3-yl)methyl)piperidin-4-yl)-3-(1*H*-indol-3-yl)propanamide (7i).** Prepared from 5-fluoro-1*H*-indole-3-carbaldehyde, *tert*-butyl piperidin-4-ylcarbamate, and (*tert*-butoxycarbonyl)-L-tryptophan according to general procedure 1 followed by general procedure 2 (38% yield over four steps). White solid. $^1$H

NMR (600 MHz, $CD_3OD$, δ): 7.57 (d, *J* = 8.1 Hz, 1H), 7.33–7.28 (comp, 2H), 7.26 (dd, *J* = 9.9, 2.3 Hz, 1H), 7.23 (s, 1H), 7.07 (ddd, *J* = 8.2, 7.1, 0.9 Hz, 1H), 7.06 (s, 1H), 6.99 (ddd, *J* = 8.0, 7.0, 0.8 Hz, 1H), 6.86 (td, *J* = 9.1, 2.5 Hz, 1H), 3.62 (s, 2H), 3.56–3.48 (comp, 2H), 3.08 (dd, *J* = 14.0, 7.2 Hz, 1H), 3.00 (dd, *J* = 14.0, 6.5 Hz, 1H), 2.86–2.68 (m, 2H), 2.18–2.02 (m, 2H), 1.72–1.62 (m, 1H), 1.51–1.14 (comp, 3H). MS (ESI) *m/z* = 434.10 $[M+H]^+$. LC-MS $^t$R (UV 214 nm): 1.035 min.

**(*S*)-2-Amino-*N*-(1-((5-bromo-1*H*-indol-3-yl)methyl)piperidin-4-yl)-3-(1*H*-indol-3-yl)propanamide (7j).** Prepared from 5-bromo-1*H*-indole-3-carbaldehyde, *tert*-butyl piperidin-4-ylcarbamate, and (*tert*-butoxycarbonyl)-L-tryptophan according to general procedure 1 followed by general procedure 2 (37% yield over four steps). Glassy solid. $^1$H NMR (400 MHz, DMSO-$d_6$, δ): 11.11 (br s, 1H), 10.80 (br s, 1H), 7.78 (d, *J* = 1.3 Hz, 1H), 7.66 (d, *J* = 7.9 Hz, 1H), 7.54 (d, *J* = 7.9 Hz, 1H), 7.31 (d, *J* = 8.5 Hz, 2H), 7.27 (d, *J* = 2.0 Hz, 1H), 7.17 (dd, *J* = 8.6, 1.7 Hz, 1H), 7.12 (d, *J* = 1.9 Hz, 1H), 7.04 (t, *J* = 7.3 Hz, 1H), 6.95 (t, *J* = 7.5 Hz, 1H), 3.55 (s, 2H), 3.53–3.46 (m, 1H), 3.39 (dd, *J* = 7.6, 5.5 Hz, 1H), 3.01 (dd, *J* = 14.0, 5.2 Hz, 1H), 2.77–2.72 (comp, 3H), 2.04 (br s, 2H), 1.95 (t, *J* = 11.1 Hz, 2H), 1.59 (t, *J* = 12.6 Hz, 2H), 1.31 (m, 2H). MS (ESI) *m/z* = 493.90 $[M+H]^+$. LC-MS $^t$R (UV 214): 1.047 min.

**(*S*)-2-Amino-3-(1*H*-indol-3-yl)-*N*-(1-((5-(trifluoromethyl)-1*H*-indol-3-yl)methyl)piperidin-4-yl)propanamide (7k).** Prepared from 5-(trifluoromethyl)-1*H*-indole-3-carbaldehyde, *tert*-butyl piperidin-4-ylcarbamate, and (*tert*-butoxycarbonyl)-L-tryptophan according to general procedure 1 followed by general procedure 2 (37% yield

over four steps). White solid. $^1$H NMR (600 MHz, $CD_3OD$, δ): 7.96 (s, 1H), 7.58 (d, *J* = 8.0 Hz, 1H), 7.49 (d, *J* = 8.5 Hz, 1H), 7.36 (d, *J* = 8.6 Hz, 1H), 7.32 (s, 1H), 7.31 (d, *J* = 8.2 Hz, 1H), 7.09–7.05 (comp, 2H), 6.99 (t, *J* = 7.5 Hz, 1H), 3.71–3.65 (m, 2H), 3.58–3.50 (comp, 2H), 3.08 (dd, *J* = 14.1, 7.2 Hz, 1H), 3.01 (dd, *J* = 14.2, 6.5 Hz, 1H), 2.81 (s, 1H), 2.74 (s, 1H), 2.12 (t, *J* = 10.9 Hz, 1H), 2.07 (t, *J* = 11.5 Hz, 1H), 1.70–1.64 (m, 1H), 1.48–1.43 (m, 1H), 1.40–1.31 (m, 1H), 1.26–1.17 (m, 1H). MS (ESI) *m/z* = 484.00 $[M+H]^+$. LC-MS $^t$R (UV 214): 0.889 min.

**(*S*)-2-Amino-*N*-(1-((5-chloro-1*H*-indol-3-yl)methyl)piperidin-4-yl)-3-(5-methoxy-1*H*-indol-3-yl)propanamide (12a).** Prepared from 5-chloro-1*H*-indole-3-carbaldehyde, *tert*-butyl piperidin-4-ylcarbamate, and 2-iodo-4-methoxyaniline according to general procedure 1 followed by general procedure 4 (4% yield over four steps). White solid. $^1$H NMR (400 MHz, $CD_3OD$, δ): 7.60 (d, *J* = 2.1 Hz, 1H), 7.31 (d, *J* = 8.6 Hz, 1H), 7.23 (s, 1H), 7.20 (d, *J* = 8.8 Hz, 1H), 7.08–7.03 (comp, 3H), 6.74 (dd, *J* = 8.8, 2.4 Hz, 1H), 3.81 (s, 3H), 3.64 (s, 2H), 3.57–3.51 (comp, 2H), 3.05 (dd, *J* = 14.0, 7.2 Hz, 1H), 2.98 (dd, *J* = 14.1, 6.4 Hz, 1H), 2.83–2.73 (br m, 2H), 2.16–2.06 (m, 2H), 1.67 (br d, *J* = 12.8 Hz, 1H), 1.47 (br d, *J* = 12.8 Hz, 1H), 1.41–1.31 (m, 1H), 1.27–1.18 (m, 1H). MS (ESI) *m/z* = 480.00 $[M+H]^+$. LC-MS $^t$R (UV 214): 1.116 min.

**(*S*)-2-Amino-*N*-(1-((5-chloro-1*H*-indol-3-yl)methyl)piperidin-4-yl)-3-(6-methoxy-1*H*-indol-3-yl)propanamide (12b).** Prepared from 5-chloro-1*H*-indole-3-carbaldehyde, *tert*-butyl piperidin-4-ylcarbamate, and 2-iodo-5-methoxyaniline according to general procedure 1 followed by general procedure 4 (5% yield over four steps). White solid. $^1$H

NMR (400 MHz, $CD_3OD$, δ): 7.60 (d, *J* = 2.0 Hz, 1H), 7.43 (d, *J* = 8.7 Hz, 1H), 7.31 (d, *J* = 8.7 Hz, 1H), 7.23 (s, 1H), 7.07 (dd, *J* = 8.6, 2.0 Hz, 1H), 6.94 (s, 1H), 6.85 (d, *J* = 2.2 Hz, 1H), 6.68 (dd, *J* = 8.7, 2.3 Hz, 1H), 3.77 (s, 3H), 3.63 (s, 2H), 3.57–3.50 (comp, 2H), 3.02 (dd, *J* = 14.1, 7.1 Hz, 1H), 2.97 (dd, *J* = 14.1, 6.6 Hz, 1H), 2.82–2.70 (br m, 2H), 2.17–2.06 (m, 2H), 1.68 (br d, *J* = 12.3 Hz, 1H), 1.48 (br d, *J* = 12.3 Hz, 1H), 1.41–1.32 (m, 1H), 1.27–1.18 (m, 1H). MS (ESI) *m/z* = 480.00 $[M+H]^+$. LC-MS $^t$R (UV 214): 1.107 min.

**(*S*)-2-Amino-*N*-(1-((5-chloro-1*H*-indol-3-yl)methyl)piperidin-4-yl)-3-(5-(trifluoromethyl)-1*H*-indol-3-yl)propanamide (12c).** Prepared from 5-chloro-1*H*-indole-3-carbaldehyde, *tert*-butyl piperidin-4-ylcarbamate, and 2-iodo-4-(trifluoromethyl)aniline according to general procedure 1 followed by general procedure 4 (2% yield over four steps). White Solid. The title compound was isolated in 93% purity, as judged by LC-MS and $^1$H NMR analysis. $^1$H NMR (400 MHz, $CD_3OD$, δ): 7.93 (s, 1H), 7.59 (d, *J* = 2.0 Hz, 1H), 7.45 (d, *J* = 8.6 Hz, 1H), 7.33 (dd, *J* = 8.5, 1.6 Hz, 1H), 7.31 (d, *J* = 8.6 Hz, 1H), 7.23 (s, 2H), 7.06 (dd, *J* = 8.6, 2.0 Hz, 1H), 3.63 (s, 2H), 3.56–3.48 (comp, 2H), 3.14–3.04 (m, 2H), 2.83–2.74 (br m, 2H), 2.14–2.05 (m, 2H), 1.64 (br d, *J* = 12.8 Hz, 1H), 1.42 (br d, *J* = 11.9 Hz, 1H), 1.36–1.31 (m, 1H), 1.24–1.14 (m, 1H). MS (ESI) *m/z* = 517.90 $[M+H]^+$. LC-MS $^t$R (UV 214): 1.310 min.

**(*S*)-2-Amino-*N*-(1-((5-chloro-1*H*-indol-3-yl)methyl)piperidin-4-yl)-3-(6-(trifluoromethyl)-1*H*-indol-3-yl)propanamide (12d).** Prepared from 5-chloro-1*H*-indole-3-carbaldehyde, *tert*-butyl piperidin-4-ylcarbamate, and 2-iodo-5-

(trifluoromethyl)aniline according to general procedure 1 followed by general procedure 4 (5% yield over four steps). White solid. $^1$H NMR (400 MHz, $CD_3OD$, δ): 7.72 (d, $J$ = 8.5 Hz, 1H), 7.63 (s, 1H), 7.59 (d, $J$ = 1.7 Hz, 1H), 7.32–7.22 (comp, 4H), 7.06 (dd, $J$ = 8.6, 1.9 Hz, 1H), 3.62 (s, 2H), 3.55–3.47 (comp, 2H), 3.12–3.02 (comp, 2H), 2.83–2.73 (br m, 2H), 2.15–2.04 (m, 2H), 1.66 (br d, $J$ = 11.9 Hz, 1H), 1.40–1.29 (m, 2H), 1.21–1.12 (m, 1H). MS (ESI) $m/z$ = 517.90 $[M+H]^+$. LC-MS $^t$R (UV 214): 1.241 min.

**(*S*)-2-Amino-*N*-(1-((5-chloro-1*H*-indol-3-yl)methyl)piperidin-4-yl)-3-(5-methyl-1*H*-indol-3-yl)propanamide (12e).** Prepared from 5-chloro-1*H*-indole-3-carbaldehyde, *tert*-butyl piperidin-4-ylcarbamate, and 2-iodo-4-methylaniline according to general procedure 1 followed by general procedure 4 (6% yield over four steps). White solid. $^1$H NMR (400 MHz, $CD_3OD$, δ): 7.60 (d, $J$ = 2.0 Hz, 1H), 7.36 (s, 1H), 7.31 (d, $J$ = 8.6 Hz, 1H), 7.22 (s, 1H), 7.19 (d, $J$ = 8.3 Hz, 1H), 7.07 (dd, $J$ = 8.6, 2.0 Hz, 1H), 7.01 (s, 1H), 6.91 (dd, $J$ = 8.3, 1.5 Hz, 1H), 3.62 (s, 2H), 3.56–3.49 (comp, 2H), 3.04 (dd, $J$ = 14.0, 7.1 Hz, 1H), 2.99 (dd, $J$ = 14.1, 6.5 Hz, 1H), 2.81–2.72 (br m, 2H), 2.39 (s, 3H), 2.14–2.05 (m, 2H), 1.66 (br d, $J$ = 12.8 Hz, 1H), 1.47 (br d, $J$ = 12.8 Hz, 1H), 1.40–1.30 (m, 1H), 1.28–1.18 (m, 1H). MS (ESI) $m/z$ = 464.00 $[M+H]^+$. LC-MS $^t$R (UV 214): 1.162 min.

**(*S*)-2-Amino-*N*-(1-((5-chloro-1*H*-indol-3-yl)methyl)piperidin-4-yl)-3-(6-methyl-1*H*-indol-3-yl)propanamide (12f).** Prepared from 5-chloro-1*H*-indole-3-carbaldehyde, *tert*-butyl piperidin-4-ylcarbamate, and 2-iodo-5-methylaniline according to general procedure 1 followed by general procedure 4 (23% yield over four steps). White solid. $^1$H NMR (400 MHz, $CD_3OD$, δ): 7.60 (d, $J$ = 2.0 Hz, 1H), 7.44 (d, $J$ = 8.2 Hz, 1H), 7.31 (d,

*J* = 8.6 Hz, 1H), 7.22 (s, 1H), 7.11 (br s, 1H), 7.06 (dd, *J* = 8.6, 2.0 Hz, 1H), 6.97 (s, 1H), 6.84 (dd, *J* = 8.2, 1.2 Hz, 1H), 3.62 (s, 2H), 3.56–3.49 (comp, 2H), 3.04 (dd, *J* = 14.0, 7.0 Hz, 1H), 2.98 (dd, *J* = 14.0, 6.6 Hz, 1H), 2.80–2.69 (br m, 2H), 2.38 (s, 3H), 2.15–2.05 (m, 2H), 1.66 (br d, *J* = 12.6 Hz, 1H), 1.46 (br d, *J* = 12.6 Hz, 1H), 1.40–1.30 (m, 1H), 1.26–1.17 (m, 1H). MS (ESI) *m/z* = 464.00 $[M+H]^+$. LC-MS $^t$R (UV 214): 1.165 min.

**(*S*)-2-Amino-3-(5-chloro-1*H*-indol-3-yl)-*N*-(1-((5-chloro-1*H*-indol-3-yl)methyl)piperidin-4-yl)propanamide (12g).** Prepared from 5-chloro-1*H*-indole-3-carbaldehyde, *tert*-butyl piperidin-4-ylcarbamate, and 4-chloro-2-iodoaniline according to general procedure 1 followed by general procedure 4 (17% yield over four steps). White solid. $^1$H NMR (400 MHz, $CD_3OD$, δ): 7.60 (d, *J* = 2.0 Hz, 1H), 7.57 (d, *J* = 2.0 Hz, 1H), 7.31 (d, *J* = 8.6 Hz, 1H), 7.27 (d, *J* = 8.7 Hz, 1H), 7.23 (s, 1H), 7.12 (s, 1H), 7.06 (dd, *J* = 8.6, 2.0 Hz, 1H), 7.03 (dd, *J* = 8.7, 2.0 Hz, 1H), 3.63 (s, 2H), 3.58–3.51 (m, 1H), 3.52–3.49 (m, 1H), 3.04 (dd, *J* = 14.1, 7.0 Hz, 1H), 2.99 (dd, *J* = 14.2, 6.5 Hz, 1H), 2.84–2.74 (br m, 2H), 2.12 (qd, *J* = 12.1, 1.8 Hz, 2H), 1.67 (br d, *J* = 12.3 Hz, 1H), 1.48 (br d, *J* = 12.3 Hz, 1H), 1.35 (qd, *J* = 11.5, 3.4 Hz, 1H), 1.23 (qd, *J* = 11.4, 3.8 Hz, 1H). MS (ESI) *m/z* = 483.90 $[M+H]^+$. LC-MS $^t$R (UV 214): 1.225 min.

**(*S*)-2-Amino-3-(6-chloro-1*H*-indol-3-yl)-*N*-(1-((5-chloro-1*H*-indol-3-yl)methyl)piperidin-4-yl)propanamide (12h).** Prepared from 5-chloro-1*H*-indole-3-carbaldehyde, *tert*-butyl piperidin-4-ylcarbamate, and 5-chloro-2-iodoaniline according to general procedure 1 followed by general procedure 4 (28% yield over four steps). White solid. $^1$H NMR (400 MHz, $CD_3OD$, δ): 7.60 (d, *J* = 2.0 Hz, 1H), 7.53 (d, *J* = 8.5 Hz, 1H),

7.32 (d, *J* = 3.3 Hz, 1H), 7.31 (d, *J* = 7.2 Hz, 1H), 7.23 (s, 1H), 7.08 (s, 1H), 7.06 (dd, *J* = 8.6, 2.0 Hz, 1H), 6.98 (dd, *J* = 8.5, 1.9 Hz, 1H), 3.63 (s, 2H), 3.56–3.48 (comp, 2H), 3.04 (dd, *J* = 14.1, 7.2 Hz, 1H), 2.99 (dd, *J* = 14.0, 6.4 Hz, 1H), 2.82–2.73 (br m, 2H), 2.15–2.06 (br m, 2H), 1.68 (br d, *J* = 12.4 Hz, 1H), 1.45 (br d, *J* = 12.4 Hz, 1H), 1.41–1.31 (m, 1H), 1.26–1.15 (m, 1H). MS (ESI) *m/z* = 484.00 $[M+H]^+$. LC-MS $^t$R (UV 214): 1.234 min.

**(*S*)-2-Amino-*N*-((1-((5-chloro-1*H*-indol-3-yl)methyl)piperidin-4-yl)methyl)-3-(1*H*-indol-3-yl)propanamide (15a).** Prepared from 5-chloro-1*H*-indole-3-carbaldehyde, *tert*-butyl (piperidin-4-ylmethyl)carbamate, and (*tert*-butoxycarbonyl)-L-tryptophan according to general procedure 1 followed by general procedure 2 (34% yield over four steps). White solid. $^1$H NMR (600 MHz, $CD_3OD$, δ): 7.62 (d, *J* = 1.8 Hz, 1H), 7.55 (dd, *J* = 6.0, 1.8 Hz, 1H), 7.34 (d, *J* = 8.6 Hz, 1H), 7.26 (s, 1H), 7.24 (dd, *J* = 6.2, 1.8 Hz, 1H), 7.10 (dd, *J* = 8.6, 1.8 Hz, 1H), 7.05 (s, 1H), 7.00–6.92 (comp, 2H), 3.68 (s, 2H), 3.58 (t, *J* = 7.8 Hz, 1H), 3.10–2.98 (comp, 3H), 2.88–2.79 (comp, 2H), 2.75 (dd, *J* = 13.5, 7.1 Hz, 1H), 1.95–1.85 (m, 2H), 1.34–0.91 (comp, 5H). MS (ESI) *m/z* = 464.00 $[M+H]^+$. LC-MS $^t$R (UV 214): 1.097 min.

**(*S*)-2-Amino-1-(7-((5-chloro-1*H*-indol-3-yl)methyl)-2,7-diazaspiro[3.5]nonan-2-yl)-3-(1*H*-indol-3-yl)propan-1-one (15b).** Prepared from 5-chloro-1*H*-indole-3-carbaldehyde, *tert*-butyl 2,7-diazaspiro[3.5]nonane-2-carboxylate, and (*tert*-butoxycarbonyl)-L-tryptophan according to general procedure 1 followed by general procedure 2 (26% yield over four steps). White solid. $^1$H NMR (600 MHz, $CD_3OD$, δ): 7.55 (d, *J* = 1.9 Hz, 1H),

7.53 (d, *J* = 7.7 Hz, 1H), 7.33 (s, 1H), 7.31 (s, 1H), 7.19 (s, 1H), 7.12–7.00 (comp, 4H), 3.58 (dd, *J* = 11.0, 4.8 Hz, 1H), 3.53 (d, *J* = 7.8 Hz, 2H), 3.40 (d, *J* = 5.8 Hz, 1H), 3.38 (d, *J* = 4.5 Hz, 1H), 3.14 (d, *J* = 10.0 Hz, 1H), 3.09 (dd, *J* = 13.4, 4.5 Hz, 1H), 2.94 (dd, *J* = 13.4, 10.9 Hz, 1H), 2.37 (br s, 1H), 2.32 (d, *J* = 8.5 Hz, 1H), 2.16 (br s, 2H), 1.57–1.45 (m, 2H), 0.88 (br s, 1H), 0.62 (br s, 1H). MS (ESI) *m/z* = 476.00 $[M+H]^+$. LC-MS $^t$R (UV 214 nm): 1.100 min.

**(*S*)-2-Amino-1-(2-((5-chloro-1*H*-indol-3-yl)methyl)-2,7-diazaspiro[3.5]nonan-7-yl)-3-(1*H*-indol-3-yl)propan-1-one (15c).** Prepared from 5-chloro-1*H*-indole-3-carbaldehyde, *tert*-butyl 2,7-diazaspiro[3.5]nonane-7-carboxylate, and (*tert*-butoxycarbonyl)-L-tryptophan according to general procedure 1 followed by general procedure 2 (34% yield over four steps). White solid. $^1$H NMR (600 MHz, $CD_3OD$, δ): 7.56 (d, *J* = 1.8 Hz, 1H), 7.51 (d, *J* = 8.1 Hz, 1H), 7.30–7.27 (comp, 2H), 7.19 (s, 1H), 7.09–7.03 (comp, 3H), 7.00 (t, *J* = 7.3 Hz, 1H), 4.10 (dd, *J* = 9.0, 6.0 Hz, 1H), 3.70 (s, 2H), 3.63–3.57 (m, 1H), 3.06–2.90 (comp, 7H), 2.82 (d, *J* = 8.0 Hz, 1H), 2.74 (d, *J* = 8.0 Hz, 1H), 1.50–1.45 (m, 1H), 1.26–1.21 (m, 1H), 1.02 (ddd, *J* = 13.4, 9.7, 3.8 Hz, 1H), 0.30 (ddd, *J* = 13.4, 9.4, 4.3 Hz, 1H). MS (ESI) *m/z* = 476.00 $[M+H]^+$. LC-MS $^t$R (UV 214): 0.869 min.

**(2*S*)-2-Amino-1-(5-((5-chloro-1*H*-indol-3-yl)methyl)hexahydropyrrolo[3,4-*c*]pyrrol-2(1*H*)-yl)-3-(1*H*-indol-3-yl)propan-1-one (15d).** Prepared from 5-chloro-1*H*-indole-3-carbaldehyde, *tert*-butyl hexahydropyrrolo[3,4-*c*]pyrrole-2(1*H*)-carboxylate, and (*tert*-butoxycarbonyl)-L-tryptophan according to general procedure 1 followed by general procedure 2 (25% yield over four steps). White solid. The title compound was isolated as

a 55:45 mixture of rotamers. $^1$H NMR (600 MHz, $CD_3OD$, δ): 7.60 (d, *J* = 1.8 Hz, 0.55H), 7.58 (d, *J* = 8.1 Hz, 0.55H), 7.55 (d, *J* = 1.8 Hz, 0.45H), 7.49 (d, *J* = 8.1 Hz, 0.45H), 7.37 (d, *J* = 8.1 Hz, 0.55H), 7.33 (d, *J* = 8.1 Hz, 0.45H), 7.30 (d, *J* = 8.6 Hz, 0.55H), 7.28 (d, *J* = 8.6 Hz, 0.45H), 7.20 (s, 0.55H), 7.17 (s, 0.45H), 7.17–6.98 (comp, 4H), 3.93 (dd, *J* = 9.4, 5.6 Hz, 0.55H), 3.90 (dd, *J* = 9.4, 5.6 Hz, 0.45H), 3.68 (s, 1H), 3.54 (d, *J* = 13.3 Hz, 0.55H), 3.51 (d, *J* = 13.3 Hz, 0.45H), 3.47–3.36 (comp, 1.55H), 3.23–3.18 (m, 1H), 3.11–2.99 (comp, 2.45H), 2.79–2.47 (comp, 4H), 2.36–2.30 (m, 1H), 2.27 (dd, *J* = 9.6, 4.4 Hz, 0.45H), 2.11–2.04 (m, 0.45H), 1.63 (dd, *J* = 9.4, 5.7 Hz, 0.55H), 1.13 (dd, *J* = 9.4, 5.2 Hz, 0.55H). MS (ESI) *m/z* = 462.00 $[M+H]^+$. LC-MS $^t$R (UV 214): 0.882 min.

**(*S*)-2-Amino-1-(2-((5-chloro-1*H*-indol-3-yl)methyl)-2,6-diazaspiro[3.4]octan-6-yl)-3-(1*H*-indol-3-yl)propan-1-one (15e).** Prepared from 5-chloro-1*H*-indole-3-carbaldehyde, *tert*-butyl 2,6-diazaspiro[3.4]octane-6-carboxylate, and (*tert*-butoxycarbonyl)-L-tryptophan according to general procedure 1 followed by general procedure 2 (31% yield over four steps). White solid. The title compound was isolated as a 50:50 mixture of rotamers. $^1$H NMR (600 MHz, $CD_3OD$, δ): 7.58 (d, *J* = 2.1 Hz, 0.5H), 7.54 (d, *J* = 2.1 Hz, 0.5H), 7.53–7.50 (m, 0.5H), 7.48–7.45 (m, 0.5H), 7.34 (d, *J* = 5.6 Hz, 0.5H), 7.32 (d, *J* = 5.6 Hz, 0.5H), 7.25–7.21 (m, 0.5H), 7.21 (s, 0.5H), 7.21–7.18 (m, 0.5H), 7.16 (s, 0.5H), 7.11–6.99 (comp, 3H), 6.97–6.89 (comp, 1H), 3.82 (d, *J* = 5.1 Hz, 0.5H), 3.79 (d, *J* = 5.1 Hz, 0.5H), 3.67 (s, 1H), 3.56 (dd, *J* = 16.1, 13.2 Hz, 1H), 3.34–3.28 (m, 0.5H), 3.27–3.19 (comp, 2H), 3.14–2.94 (comp, 4.5H), 2.67 (d, *J* = 7.7 Hz, 0.5H), 2.53 (d, *J* =

8.2 Hz, 0.5H), 2.49–2.44 (comp, 1H), 2.27–2.19 (m, 0.5H), 2.06 (d, *J* = 8.0 Hz, 0.5H), 1.79–1.40 (comp, 2H). MS (ESI) *m/z* = 462.00 $[M+H]^+$. LC-MS $^t$R (UV 214): 0.868 min.

**(*S*)-2-Amino-1-(1-((5-chloro-1*H*-indol-3-yl)methyl)-1,7-diazaspiro[3.5]nonan-7-yl)-3-(1*H*-indol-3-yl)propan-1-one (15f).** Prepared from 5-chloro-1*H*-indole-3-carbaldehyde, *tert*-butyl 1,7-diazaspiro[3.5]nonane-7-carboxylate, and (*tert*-butoxycarbonyl)-L-tryptophan according to general procedure 1 followed by general procedure 2 (17% yield over four steps). White solid. The title compound was isolated as a 60:40 mixture of rotamers. $^1$H NMR (600 MHz, DMSO-$d_6$, δ): 10.97 (s, 1H), 10.88 (s, 0.6H), 10.82 (s, 0.4H), 7.60 (d, *J* = 1.6 Hz, 0.4H), 7.58 (d, *J* = 1.6 Hz, 0.6H), 7.54 (d, *J* = 7.8 Hz, 0.6H), 7.47 (d, *J* = 7.8 Hz, 0.4H), 7.33 (d, *J* = 8.6 Hz, 0.6H), 7.32 (d, *J* = 8.2 Hz, 0.4H), 7.31 (d, *J* = 8.6 Hz, 0.4H), 7.27 (d, *J* = 8.2 Hz, 0.6H), 7.22 (d, *J* = 1.6 Hz, 0.4H), 7.18 (d, *J* = 1.6 Hz, 0.6H), 7.13 (d, *J* = 1.6 Hz, 0.4H), 7.12 (d, *J* = 1.6 Hz, 0.6H), 7.07–7.02 (comp, 2H), 7.00 (t, *J* = 7.5 Hz, 0.6H), 6.96 (t, *J* = 7.5 Hz, 0.4H), 4.32 (t, *J* = 14.3 Hz, 1H), 4.02 (dd, *J* = 8.2, 6.2 Hz, 0.6H), 3.92 (t, *J* = 6.5 Hz, 0.4H), 3.78 (d, *J* = 13.6 Hz, 0.4H), 3.65 (s, 0.6H), 3.61 (d, *J* = 13.6 Hz, 0.6H), 3.40–3.29 (comp, 0.8H), 3.01 (t, *J* = 7.3 Hz, 0.6H), 2.94–2.78 (comp, 3H), 2.74 (t, *J* = 12.6 Hz, 0.6H), 2.73–2.69 (m, 0.4H), 2.61 (t, *J* = 12.6 Hz, 0.4H), 2.43–2.29 (comp, 1H), 2.21–1.91 (br s, 2H), 1.80–1.65 (comp, 3H), 1.61–1.55 (m, 1H), 1.47 (td, *J* = 12.4, 4.8 Hz, 0.4H), 1.30–1.20 (comp, 1H), 0.94 (td, *J* = 12.4, 4.3 Hz, 0.6H), 0.25 (td, *J* = 13.0, 4.0 Hz, 0.6H). MS (ESI) *m/z* = 476.00 $[M+H]^+$. LC-MS $^t$R (UV 214): 1.123 min.

**(2*S*)-2-Amino-1-(5-((5-chloro-1*H*-indol-3-yl)methyl)hexahydropyrrolo[3,4-*c*]pyrrol-2(1*H*)-yl)-3-(6-methyl-1*H*-indol-3-yl)propan-1-one (16).** Prepared from 5-chloro-1*H*-indole-3-carbaldehyde, *tert*-butyl hexahydropyrrolo[3,4-*c*]pyrrole-2(1*H*)-carboxylate, and 2-iodo-5-methylaniline according to general procedure 1 followed by general procedure 4 (27% yield over four steps). White solid. The title compound was isolated as a 60:40 mixture of rotamers. $^1$H NMR (400 MHz, $CD_3OD$, δ): 7.58 (d, *J* = 1.9 Hz, 0.6H), 7.54 (d, *J* = 1.9 Hz, 0.4H), 7.44 (d, *J* = 8.1 Hz, 0.6H), 7.36 (d, *J* = 8.1 Hz, 0.4H), 7.31 (d, *J* = 8.6 Hz, 0.6H), 7.28 (d, *J* = 8.6 Hz, 0.4H), 7.18 (s, 0.6H), 7.16 (s, 0.4H), 7.13–7.12 (m, 1H), 7.07–7.02 (m, 1H), 7.02 (s, 0.6H), 6.97 (s, 0.4H), 6.89 (dd, *J* = 8.1, 1.0 Hz, 0.6H), 6.84 (dd, *J* = 8.1, 1.0 Hz, 0.4H), 3.89 (dd, *J* = 9.2, 5.8 Hz, 0.6H), 3.85 (dd, *J* = 9.1, 5.7 Hz, 0.4H), 3.66 (s, 0.8H), 3.50 (s, 1.2H), 3.91–3.83 (comp, 1.6H), 3.24–3.19 (m, 1H), 3.09–2.97 (comp, 2.4H), 2.80–2.70 (m, 1H), 2.66–2.48 (comp, 3.4H), 2.40 (s, 1.2H), 2.37 (s, 1.8H), 2.32–2.23 (m, 0.6H), 2.24 (dd, *J* = 9.7, 4.5 Hz, 0.4H), 2.15–2.08 (m, 0.4H), 1.62 (dd, *J* = 9.1, 5.9 Hz, 0.6H), 1.08 (dd, *J* = 8.9, 5.1 Hz, 0.6H). MS (ESI) *m/z* = 476.00 $[M+H]^+$. LC-MS $^t$R (UV 214): 1.004 min.

**(2*S*)-2-Amino-3-(6-chloro-1*H*-indol-3-yl)-1-(5-((5-chloro-1*H*-indol-3-yl)methyl)hexahydropyrrolo[3,4-*c*]pyrrol-2(1*H*)-yl)propan-1-one (17).** Prepared from 5-chloro-1*H*-indole-3-carbaldehyde, *tert*-butyl hexahydropyrrolo[3,4-*c*]pyrrole-2(1*H*)-carboxylate, and 5-chloro-2-iodoaniline according to general procedure 1 followed by general procedure 4 (37% yield over four steps). White solid. The title compound was isolated as a 60:40 mixture of rotamers. $^1$H NMR (400 MHz, $CD_3OD$, δ): 7.60 (d, *J* = 1.9 Hz, 0.6H), 7.55 (d, *J* = 1.9 Hz, 0.4H), 7.51 (d, *J* = 8.5 Hz, 0.6H), 7.44 (d, *J* = 8.5 Hz,

0.4H), 7.37 (d, *J* = 1.7 Hz, 0.6H), 7.33 (d, *J* = 1.7 Hz, 0.4H), 7.29 (d, *J* = 8.5 Hz, 0.6H), 7.28 (d, *J* = 8.5 Hz, 0.4H), 7.20 (s, 0.6H), 7.17 (s, 0.4H), 7.14 (s, 0.6H), 7.09 (s, 0.4H), 7.06–7.01 (comp, 1.6H), 6.98 (dd, *J* = 8.5, 1.8 Hz, 0.4H), 3.89–3.85 (m, 1H), 3.68 (s, 0.8H), 3.54 (d, *J* = 3.4 Hz, 1H), 3.50–3.39 (comp, 1.6H), 3.26–3.12 (comp, 1.6H), 3.04–3.01 (comp, 2H), 2.81–2.74 (m, 1H), 2.67–2.52 (comp, 3.2H), 2.42–2.39 (m, 0.4H), 2.35–2.27 (comp, 0.8H), 2.23–2.17 (m, 0.4H), 1.64 (dd, *J* = 9.6, 5.6 Hz, 0.6H), 1.14 (dd, *J* = 8.3, 4.3 Hz, 0.6H). MS (ESI) *m/z* = 495.90 $[M+H]^+$. LC-MS $^t$R (UV 214): 1.019 min.

**(*S*)-2-Amino-1-(1-((5-chloro-1*H*-indol-3-yl)methyl)-1,7-diazaspiro[3.5]nonan-7-yl)-3-(6-methyl-1*H*-indol-3-yl)propan-1-one (18).** Prepared from 5-chloro-1*H*-indole-3-carbaldehyde, *tert*-butyl 1,7-diazaspiro[3.5]nonane-7-carboxylate, and 2-iodo-5-methylaniline according to general procedure 1 followed by general procedure 4 (13% yield over four steps). White solid. The title compound was isolated as a 60:40 mixture of rotamers. $^1$H NMR (400 MHz, DMSO-$d_6$, δ): 10.97 (br s, 1H), 10.70 (br s, 0.6H), 10.65 (br s, 0.4H), 7.60 (d, *J* = 1.6 Hz, 0.4H), 7.55 (d, *J* = 1.8 Hz, 0.6H), 7.39 (d, *J* = 8.1 Hz, 0.6H), 7.35–7.30 (comp, 1.4H), 7.21 (d, *J* = 1.6 Hz, 0.4H), 7.18 (d, *J* = 1.9 Hz, 0.6H), 7.10 (s, 0.4H), 7.07–7.02 (comp, 2.6H), 6.82–6.79 (m, 1H), 4.35–4.29 (m, 1H), 4.01 (dd, *J* = 8.2, 6.4 Hz, 0.6H), 3.91 (t, *J* = 6.4 Hz, 0.4H), 3.77 (d, *J* = 12.2 Hz, 0.4H), 3.65 (s, 1H), 3.59 (d, *J* = 12.7 Hz, 0.6H), 3.02 (t, *J* = 6.9 Hz, 1H), 2.90–2.59 (comp, 5H), 2.46–2.40 (comp, 1H), 2.28 (s, 3H), 1.83–1.67 (comp, 3H), 1.61–1.55 (comp, 1H), 1.28–1.24 (comp, 0.8H), 0.99–0.91 (m, 0.6H), 0.27–0.19 (m, 0.6H). MS (ESI) *m/z* = 490.00 $[M+H]^+$. LC-MS $^t$R (UV 214): 0.939 min.

**(*S*)-2-Amino-3-(6-chloro-1*H*-indol-3-yl)-1-(1-((5-chloro-1*H*-indol-3-yl)methyl)-1,7-diazaspiro[3.5]nonan-7-yl)propan-1-one (19).** Prepared from 5-chloro-1*H*-indole-3-carbaldehyde, *tert*-butyl 1,7-diazaspiro[3.5]nonane-7-carboxylate, and 5-chloro-2-iodoaniline according to general procedure 1 followed by general procedure 4 (7% yield over four steps). White solid. The title compound was isolated as a 60:40 mixture of rotamers. $^1$H NMR (400 MHz, DMSO-$d_6$, δ): 11.05 (br s, 0.6H), 10.98 (br s, 1.4H), 7.59 (br s, 1H), 7.52 (d, $J$ = 8.5 Hz, 0.6H), 7.47 (d, $J$ = 8.5 Hz, 0.4H), 7.36–7.30 (comp, 2H), 7.22–7.19 (comp, 2H), 7.06–6.96 (comp, 2H), 4.30 (t, $J$ = 12.0 Hz, 1H), 4.04 (t, $J$ = 6.9 Hz, 0.6H), 3.97 (t, $J$ = 6.9 Hz, 0.4H), 3.77 (d, $J$ = 12.9 Hz, 0.4H), 3.66 (s, 1H), 3.60 (d, $J$ = 12.9 Hz, 0.6H), 3.03 (t, $J$ = 6.4 Hz, 1H), 2.92–2.72 (comp, 4.6H), 2.64–2.58 (m, 0.4H), 2.43–2.31 (comp, 1H), 1.81–1.67 (comp, 3H), 1.59 (d, $J$ = 12.2 Hz, 1H), 1.51–1.44 (m, 0.4H), 1.34 (d, $J$ = 12.4 Hz, 0.4H), 0.89 (td, $J$ = 12.9, 4.6 Hz, 0.6H), 0.23 (td, $J$ = 12.9, 4.2 Hz, 0.6H). MS (ESI) $m/z$ = 510.00 $[M+H]^+$. LC-MS $^t$R (UV 214): 0.962 min.

**Pan Assay Interference Compounds (PAINS).** Certain 3-substituted indoles, including the 3-alkylaminoindoles reported here, are described as pan assay interference (PAINS) molecules.[38] Indeed, such compounds can serve as precursors to reactive vinylogous imine/iminium intermediates upon elimination of the amine. While we have observed some early examples of this behavior under acidic conditions (not reported here), the indoles presented in this manuscript are chemically robust under the conditions of the assays in which they have been assessed, to include the nucleotide exchange assay and the fluorescence polarization (FP) assay reported previously.[24] The results obtained from these two orthogonal assays, coupled with the multiple X-ray co-crystal structures and the loss of activity observed upon mutation of specific amino acid residues in the binding pocket,[24] confirm that the activity of these compounds is due to a distinct, non-covalent binding event.

## ■ ASSOCIATED CONTENT

**Supporting Information.** The Supporting Information associated with this manuscript is available free of charge on the ACS Publications website. Files include:

Biochemical and cellular assay conditions; quantification tables for western blotting experiments; molecular modeling studies; details regarding protein expression and purification; details regarding crystallization, X-ray data collection, structure solution, and refinement; and a table containing X-ray data collection and refinement statistics.

Molecular formula strings (CSV)

**Accession Codes.** The structures of compound **4c** (PDB ID code 4NYJ) and compound **4k** (PDB ID code 4NYM) have been reported previously.[24]

Compound **12e** (PDB ID code 6BVL)

Compound **12f** (PDB ID code 6BVK)

Compound **12g** (PDB ID code 6BVJ)

Compound **12h (**PDB ID code 6BVI)

Compound **15d** (PDB ID code 6BVM)

Authors will release the atomic coordinates and experimental data upon article publication.

## ■ AUTHOR INFORMATION

**Corresponding Author.**

*E-mail: stephen.fesik@vanderbilt.edu.

Phone: +1 (615) 322-6303

Fax: +1 (615) 875-3236

**Present Addresses.**

[†]R.N.D.: Lipscomb University, Nashville, TN, USA

[‡]P.A.P.: PharmAgra Labs, Brevard, NC, USA

[⊥]J.P.K.: Truetiva, Inc., Monterey, CA, USA

[Ω]M.C.B.: Northwestern University Feinberg School of Medicine, Chicago, IL, USA

[¶]T.S.: TerSera Therapeutics, Lake Forest, IL, USA

[£]O.W.R.: The Institute of Cancer Research, London, UK

**Author Contributions.**

[#]J.R.A. and T.R.H. contributed equally to this work. All authors have given approval to the final version of this manuscript.

**Notes.**

RAS activator compounds have been licensed to Boehringer Ingelheim.

## ■ ACKNOWLEDGMENTS

Funding for this work came from the following sources:

U. S. National Institutes of Health, NIH Director's Pioneer Award (DP1OD006933/DP1CA174419) to S. W. Fesik

Lustgarten Foundation Research Investigator Grant to S. W. Fesik

National Cancer Institute SPORE Grant in GI Cancer (5P50A095103-09) to R. J. Coffey

The authors would like to thank the following core facilities for their contributions to this work:

Experiments were performed in the Vanderbilt High Throughput Screening (HTS) Core Facility with assistance provided by C. David Weaver, Paige Vinson, Chris Farmer, and Corbin Whitwell. The HTS Core receives support from the Vanderbilt Institute of Chemical Biology and the Vanderbilt Ingram Cancer Center (P30 CA68485).

The Vanderbilt University Biomolecular NMR Facility for instrumentation. This facility receives support from an NIH SIG Grant (1S-10RR025677-01) and Vanderbilt University matching funds.

The U.S. Department of Energy, Office of Science, Office of Basic Energy Sciences for use of the Advanced Photon Source (Contract: DE-AC02-06CH11357).

## ■ ABBREVIATIONS USED

PyBOP, (benzotriazol-1-yloxy)tripyrrolidinophosphonium hexafluorophosphate; HATU, 1-[bis(dimethylamino)methylene]-1*H*-1,2,3-triazolo[4,5-*b*]pyridinium 3-oxid

hexafluorophosphate; $Et_2O$, diethyl ether; *i*-$Pr_2NEt$, *N*,*N*-diisopropylethylamine; EGF, epidermal growth factor; EtOH, ethanol; EtOAc, ethyl acetate; ERK1/2, extracellular regulated kinases 1 and 2; GRB2, growth factor receptor bound protein 2; GEF, guanine nucleotide exchange factor; LE, ligand efficiency; LipE, lipophilic efficiency; MAPK, mitogen-activated protein kinase; $Pd(OAc)_2$, palladium(II) acetate; $N_2$, nitrogen; pERK1/2, phosphorylated ERK1/2; KOH, potassium hydroxide; RTK, receptor tyrosine kinase; $NaHCO_3$, sodium bicarbonate; NaCl, sodium chloride; $Na_2SO_4$, sodium sulfate; $NaBH(OAc)_3$, sodium triacetoxyborohydride; SOS1, son of sevenless homologue 1; $H_2O$, water.

## ■ REFERENCES

1. Colicelli, J. Human RAS Superfamily Proteins and Related GTPases. *Sci. STKE* **2004**, *2004* (250), re13.

2. Mitin, N.; Rossman, K. L.; Der, C. J. Signaling Interplay in Ras Superfamily Function. *Curr. Biol.* **2005**, *15* (14), R563–R574.

3. Pulgar, T. G. D.; Lacal, J. C. GTPase. In *Encyclopedia of Cancer*; Schwab, M., Ed.; Springer Berlin Heidelberg: Berlin, Heidelberg, 2011; pp 1609–1613.

4. Downward, J. Regulatory Mechanisms for *ras* Proteins. *BioEssays* **1992**, *14* (3), 177–184.

5. Boguski, M. S.; McCormick, F. Proteins Regulating Ras and Its Relatives. *Nature* **1993**, *366* (6456), 643–654.

6. Vetter, I. R.; Wittinghofer, A. The Guanine Nucleotide-Binding Switch in Three Dimensions. *Science* **2001**, *294* (5545), 1299–1304.

7. Bos, J. L.; Rehmann, H.; Wittinghofer, A. GEFs and GAPs: Critical Elements in the Control of Small G Proteins. *Cell* **2007**, *129* (5), 865–877.

8. Vigil, D.; Cherfils, J.; Rossman, K. L.; Der, C. J. Ras Superfamily GEFs and GAPs: Validated and Tractable Targets for Cancer Therapy? *Nat. Rev. Cancer* **2010**, *10* (12), 842–857.

9. Hanahan, D.; Weinberg, R. A. The Hallmarks of Cancer. *Cell* **2000**, *100* (1), 57–70.

10. Hanahan, D.; Weinberg, R. A. Hallmarks of Cancer: The Next Generation. *Cell* **2011**, *144* (5), 646–674.

11. Pylayeva-Gupta, Y.; Grabocka, E.; Bar-Sagi, D. RAS Oncogenes: Weaving a Tumorigenic Web. *Nat. Rev. Cancer* **2011**, *11* (11), 761–774.

12. Prior, I. A.; Lewis, P. D.; Mattos, C. A Comprehensive Survey of Ras Mutations in Cancer. *Cancer Res.* **2012**, *72* (10), 2457–2467.

13. Cox, A. D.; Fesik, S. W.; Kimmelman, A. C.; Luo, J.; Der, C. J. Drugging the Undruggable RAS: Mission Possible? *Nat. Rev. Drug Discovery* **2014**, *13* (11), 828–851.

14. Waldmann, H.; Karaguni, I.-M.; Carpintero, M.; Gourzoulidou, E.; Herrmann, C.; Brockmann, C.; Oschkinat, H.; Müller, O. Sulindac-Derived Ras Pathway Inhibitors Target the Ras–Raf Interaction and Downstream Effectors in the Ras Pathway. *Angew. Chem., Int. Ed.* **2004**, *43* (4), 454–458.

15. Rosnizeck, I. C.; Graf, T.; Spoerner, M.; Tränkle, J.; Filchtinski, D.; Herrmann, C.; Gremer, L.; Vetter, I. R.; Wittinghofer, A.; König, B.; Kalbitzer, H. R. Stabilizing a Weak Binding State for Effectors in the Human Ras Protein by Cyclen Complexes. *Angew. Chem., Int. Ed.* **2010**, *49* (22), 3830–3833.

16. Maurer, T.; Garrenton, L. S.; Oh, A.; Pitts, K.; Anderson, D. J.; Skelton, N. J.; Fauber, B. P.; Pan, B.; Malek, S.; Stokoe, D.; Ludlam, M. J. C.; Bowman, K. K.; Wu, J.; Giannetti, A. M.; Starovasnik, M. A.; Mellman, I.; Jackson, P. K.; Rudolph, J.; Wang, W.; Fang, G. Small-Molecule Ligands Bind to a Distinct Pocket in Ras and Inhibit SOS-Mediated Nucleotide Exchange Activity. *Proc. Natl. Acad. Sci. U.S.A.* **2012**, *109* (14), 5299–5304.

17. Sun, Q.; Burke, J. P.; Phan, J.; Burns, M. C.; Olejniczak, E. T.; Waterson, A. G.; Lee, T.; Rossanese, O. W.; Fesik, S. W. Discovery of Small Molecules That Bind to K-Ras and Inhibit Sos-Mediated Activation. *Angew. Chem., Int. Ed.* **2012**, *51* (25), 6140–6143.

18. Wang, W.; Fang, G.; Rudolph, J. Ras Inhibition Via Direct Ras Binding—Is There a Path Forward? *Bioorg. Med. Chem. Lett.* **2012**, *22* (18), 5766–5776.

19. Hocker, H. J.; Cho, K.-J.; Chen, C.-Y. K.; Rambahal, N.; Sagineedu, S. R.; Shaari, K.; Stanslas, J.; Hancock, J. F.; Gorfe, A. A. Andrographolide Derivatives Inhibit Guanine Nucleotide Exchange and Abrogate Oncogenic Ras Function. *Proc. Natl. Acad. Sci. U.S.A.* **2013**, *110* (25), 10201–10206.

20. Ostrem, J. M.; Peters, U.; Sos, M. L.; Wells, J. A.; Shokat, K. M. K-Ras(G12C) Inhibitors Allosterically Control GTP Affinity and Effector Interactions. *Nature* **2013**, *503* (7477), 548–551.

21. Shima, F.; Yoshikawa, Y.; Ye, M.; Araki, M.; Matsumoto, S.; Liao, J.; Hu, L.; Sugimoto, T.; Ijiri, Y.; Takeda, A.; Nishiyama, Y.; Sato, C.; Muraoka, S.; Tamura, A.; Osoda, T.; Tsuda, K.-i.; Miyakawa, T.; Fukunishi, H.; Shimada, J.; Kumasaka, T.; Yamamoto, M.; Kataoka, T. *In Silico* Discovery of Small-Molecule Ras Inhibitors That

Display Antitumor Activity by Blocking the Ras–Effector Interaction. *Proc. Natl. Acad. Sci. U.S.A.* **2013**, *110* (20), 8182–8187.

22. Spiegel, J.; Cromm, P. M.; Zimmermann, G.; Grossmann, T. N.; Waldmann, H. Small-Molecule Modulation of Ras Signaling. *Nat. Chem. Biol.* **2014**, *10* (8), 613–622.

23. Leshchiner, E. S.; Parkhitko, A.; Bird, G. H.; Luccarelli, J.; Bellairs, J. A.; Escudero, S.; Opoku-Nsiah, K.; Godes, M.; Perrimon, N.; Walensky, L. D. Direct Inhibition of Oncogenic KRAS by Hydrocarbon-Stapled SOS1 Helices. *Proc. Natl. Acad. Sci. U.S.A.* **2015**, *112* (6), 1761–1766.

24. Burns, M. C.; Sun, Q.; Daniels, R. N.; Camper, D.; Kennedy, J. P.; Phan, J.; Olejniczak, E. T.; Lee, T.; Waterson, A. G.; Rossanese, O. W.; Fesik, S. W. Approach for Targeting Ras With Small Molecules That Activate SOS-Mediated Nucleotide Exchange. *Proc. Natl. Acad. Sci. U.S.A.* **2014**, *111* (9), 3401–3406.

25. Winter, J. J. G.; Anderson, M.; Blades, K.; Brassington, C.; Breeze, A. L.; Chresta, C.; Embrey, K.; Fairley, G.; Faulder, P.; Finlay, M. R. V.; Kettle, J. G.; Nowak, T.; Overman, R.; Patel, S. J.; Perkins, P.; Spadola, L.; Tart, J.; Tucker, J. A.; Wrigley, G. Small Molecule Binding Sites on the Ras:SOS Complex Can Be Exploited for Inhibition of Ras Activation. *J. Med. Chem.* **2015**, *58* (5), 2265–2274.

26. Ostrem, J. M. L.; Shokat, K. M. Direct Small-Molecule Inhibitors of KRAS: From Structural Insights to Mechanism-Based Design. *Nat. Rev. Drug Discovery* **2016**, *15* (11), 771–785.

27. Margarit, S. M.; Sondermann, H.; Hall, B. E.; Nagar, B.; Hoelz, A.; Pirruccello, M.; Bar-Sagi, D.; Kuriyan, J. Structural Evidence for Feedback Activation by Ras·GTP of the Ras-Specific Nucleotide Exchange Factor SOS. *Cell* **2003**, *112* (5), 685–695.

28. Howes, J. E.; Akan, D. T.; Burns, M. C.; Rossanese, O. W.; Waterson, A. G.; Fesik, S. W. Small Molecule-Mediated Activation of RAS Elicits Biphasic Modulation of Phospho-ERK Levels That Are Regulated Through Negative Feedback on SOS1. *Mol. Cancer Ther.* **2018**, *17* (5), 1051–1060.

29. Jia, Y.; Zhu, J. Palladium-Catalyzed, Modular Synthesis of Highly Functionalized Indoles and Tryptophans by Direct Annulation of Substituted *o*-Haloanilines and Aldehydes. *J. Org. Chem.* **2006**, *71* (20), 7826–7834.

30. Burns, M. C.; Howes, J. E.; Sun, Q.; Little, A. J.; Camper, D. V.; Abbott, J. R.; Phan, J.; Lee, T.; Waterson, A. G.; Rossanese, O. W.; Fesik, S. W. High-Throughput Screening Identifies Small Molecules That Bind to the RAS:SOS:RAS Complex and Perturb RAS Signaling. *Anal. Biochem.* **2018**, *548*, 44–52.

31. In a prevous publication (Ref. 24), compounds **4k**, **7d**, and **7h** were reported to have $EC_{50}$ values of >100, 14.0, and 25.1 μM, respectively. The $EC_{50}$ values reported for these compounds in this manuscript represent averages incorporating more runs of the nucleotide exchange assay.

32. Waring, M. J. Lipophilicity in Drug Discovery. *Expert Opin. Drug Discovery* **2010**, *5* (3), 235–248.

33. Arnott, J. A.; Planey, S. L. The Influence of Lipophilicity in Drug Discovery and Design. *Expert Opin. Drug Discovery* **2012**, *7* (10), 863–875.

34. Hopkins, A. L.; Keserü, G. M.; Leeson, P. D.; Rees, D. C.; Reynolds, C. H. The Role of Ligand Efficiency Metrics in Drug Discovery. *Nat. Rev. Drug Discovery* **2014**, *13* (2), 105–121.

35. Chang, C. A.; Chen, W.; Gilson, M. K. Ligand Configurational Entropy and Protein Binding. *Proc. Natl. Acad. Sci. U.S.A.* **2007**, *104* (5), 1534–1539.

36. Zheng, Y.; Tice, C. M.; Singh, S. B. The Use of Spirocyclic Scaffolds in Drug Discovery. *Bioorg. Med. Chem. Lett.* **2014**, *24* (16), 3673–3682.

37. Fang, Z.; Song, Y.; Zhan, P.; Zhang, Q.; Liu, X. Conformational Restriction: An Effective Tactic in 'Follow-On'-Based Drug Discovery. *Future Med. Chem.* **2014**, *6* (8), 885–901.

38. Baell, J. B.; Holloway, G. A. New Substructure Filters for Removal of Pan Assay Interference Compounds (PAINS) from Screening Libraries and for Their Exclusion in Bioassays. *J. Med. Chem.* **2010**, *53* (7), 2719–2740.

## ■ TABLE OF CONTENTS GRAPHIC